J. Helminthol. Soc. Wash.
64(1), 1997 pp. 59–95

Ultrastructure of the Lesion Nematode, *Pratylenchus penetrans* (Nemata: Pratylenchidae)*

BURTON Y. ENDO,[1] ULRICH ZUNKE,[2] AND WILLIAM P. WERGIN[1]

[1] U.S. Department of Agriculture, Agricultural Research Service, Plant Sciences Institute, Nematology Laboratory, Beltsville, Maryland 20705-2350 and

[2] Universtät Hamburg, Institut für Angewandte Botanik, Marseiller Str. 7, 20355, Hamburg, Germany

ABSTRACT: Various stages of a lesion nematode, *Pratylenchus penetrans* (Cobb, 1917) Sher and Allen, 1953, were observed with transmission electron microscopy and low-temperature scanning electron microscopy (LTSEM) to elucidate the structural anatomy of the esophagus, intestine, and reproductive system. The lumen of the esophagus is circular through the procorpus and triradiate in the metacorpus where it is part of the metacorpus pump valve. A pair of esophageal lumen branches terminate as quadriradiate valves in the subventral gland ampullae. The central lumen extends posteriad to become part of the esophago-intestinal valve. The enlarged intestinal lumen is delineated by scattered evaginated membranes of the epithelial cells. The lumen may be occluded during nonfeeding periods or when the intestine becomes compressed by the reproductive organs. The testis contains spermatocytes with membrane-bound nuclei that transform into amoeboid spermatids with electron-opaque, nonmembrane-bound nuclei surrounded by fibrous bodies. Spermatozoa with irregular clumps of nonmembrane-bound chromatin surrounded by mitochondria as well as residual fibrous bodies were found in seminal vesicles and vas deferens of males and in spermathecae of female gonads. The ultrastructure of the male and female reproductive organs is compared to similar features observed with light microscopy and LTSEM.

KEY WORDS: anatomy, esophagus, fine structure, gonad, lesion nematode, oocyte, *Pratylenchus penetrans*, sperm, ultrastructure.

Lesion nematodes (*Pratylenchus* spp.) are recognized worldwide as one of the major deterrents to crop production. These nematodes are migratory ecto- and endoparasites that cause severe root damage on a wide range of crops while feeding primarily in the cortex and secondarily on root hairs as an ectoparasite (Dropkin, 1989; Zunke, 1990a). The mode of penetration, disease symptoms, and pathogenesis of *Pratylenchus* spp., either as lone parasite or in conjunction with other pathogens, have been reviewed previously (Dropkin, 1989). The ecto- and endoparasitic feeding behavior of *P. penetrans* (Cobb, 1917) Sher and Allen, 1953, on roots in culture was observed with the use of video-enhanced contrast light microscopy. Feeding activities were separated into 4 phases consisting of stylet probing, cell penetration, salivation, and food ingestion (Zunke, 1987, 1990a, 1990b; Zunke and Institut für den Wissenschaftlichen Film, 1988; Zunke and Perry, 1992). Parasitized cortical cells had hypertrophied nuclei and protoplast separation from cell walls. Neighboring cells were also affected by components of salivation, which penetrated adjacent cell walls through plasmodesmata (Zunke, 1990b). In a related ultrastructural study of the root pathology of *P. penetrans*, plant cells that had been fed upon showed an increase in tannins, degeneration of mitochondria, numerous ribosomes, and no internal membrane structure (Townshend et al., 1989). Histological studies showed that nematode feeding was associated with polyphenolic oxidase production and tannin deposition (Townshend and Stobbs, 1981). Studies on the ultrastructure of the esophageal region, particularly on the secretory granules, are lacking for *Pratylenchus* spp. Major ultrastructural studies on the anterior region of *Pratylenchus* have emphasized the tacto- and chemosensory anatomy of the sensilla in the anterior cephalic region (De Grisse, 1977; Trett and Perry, 1985). Similar ultrastructural studies have been conducted on related tylenchid nematodes such as *Ditylenchus dipsaci* (Kühn, 1957) Filijev, 1936, *Heterodera* spp., and *Meloidogyne* spp., with emphasis on sensory systems (Yuen, 1967; Baldwin and Hirschmann, 1973, 1975; Wergin and Endo, 1976; De Grisse, 1977; Endo and Wergin, 1977,

* Mention of a trade name, warranty, proprietary product, or vendor does not constitute a guarantee of a product and does not imply its approval to the exclusion of other products or vendors that may also be suitable.

1988; Endo, 1980; Coomans and De Grisse, 1981) and on feeding activity related to the esophageal glands (Bird, 1967, 1968; Bird and Saurer, 1967; Yuen, 1968; Rumpenhorst, 1984; Wyss et al., 1984; Atkinson et al., 1988; Atkinson and Harris, 1989; Hussey, 1989; Hussey and Mims, 1990; Hussey et al., 1990; Zunke and Perry, 1992; Wyss, 1992; Endo, 1993; Davis et al., 1994). Studies on embryogenesis and postembryogenesis in several *Pratylenchus* spp. indicated that 2 gonads developed to the fourth molt, after which the posterior gonad deteriorated (Roman and Hirschmann, 1969). Ultrastructural studies of the reproductive system of plant parasitic nematodes were reviewed in a comprehensive study of spermatogenesis and sperm ultrastructure in cyst nematodes, including *Globodera rostochiensis* (Wollenweber, 1923) Behrens, 1975, *G. virginiae* (Miller and Gray, 1968) Behrens, 1975, *Heterodera schachtii* Schmidt, 1871, and *H. avenae* Wollenweber, 1924 (Shepherd and Kempton, 1973). Fine structure of developing sperm of *Ekphymatodera thomasoni* Baldwin et al., 1989, was compared with other Heteroderinae as part of a study to recognize diversity and phytogenetically informative characters within the subfamily (Cares and Baldwin, 1994a, b). Ultrastructural observations were made on the male copulatory organs of *P. penetrans* (Wen and Chen, 1976; Mai et al., 1977).

Transmission and scanning electron micrographs and their interpretations can be a foundation for subsequent biological and molecular approaches to studies of nematode feeding processes and their disruption. The identification and labeling of secretory granules, as determined with other species (Atkinson et al., 1988; Davis et al., 1994; Goverse et al., 1994), may provide ways of understanding the processes of the digestive system and the manner in which stylet secretions interact with host cells. In addition, ultrastructure of characters of lesion nematodes can contribute to studies on phylogenetic relationships among plant-parasitic nematodes.

In this study, we examined the ultrastructural anatomy of *P. penetrans* at various stages of development. Emphasis was on the alimentary canal in relation to the stylet, esophagus, and intestine and on the structure of male and female gonads.

Materials and Methods

Infective and parasitic stages of *P. penetrans* were obtained from root cultures of corn (*Zea mays* L. 'Iochief') grown in Gamborg's B-5 medium without cytokinins or auxins (Gamborg et al., 1976). Adults and juveniles were collected from infected root pieces that were incubated in water. The samples were prepared for electron microscopy as previously described (Endo and Wergin, 1973; Wergin and Endo, 1976). Nematodes embedded in 2% water agar slices or in infected root were fixed in buffered 3% glutaraldehyde (0.05 M phosphate buffer, pH 6.8) at 22°C for 1.5 hr, washed for 1 hr in 6 changes of buffer, postfixed in buffered 2% osmium tetroxide for 2 hr, dehydrated in an acetone series, and infiltrated with a low-viscosity embedding medium (Spurr, 1969). Silver-gray sections were cut on an ultramicrotome with a diamond knife and mounted on uncoated 75- × -300-mesh copper grids. The sections were stained with uranyl acetate and lead citrate and viewed in a Philips 301 or 400T electron microscope operating at 60 kV with a 20-μm objective aperture.

For low-temperature scanning electron microscopy (LTSEM), samples of *P. penetrans* were obtained from the cultures already above and prepared as previously described (Wergin et al., 1993). Specimens were placed on the surface of a flat specimen holder or in a 1-mm^3 vertical chamber formed by slots traversing the 2 halves of a closed, hinged, 24-carat gold holder. The specimen holders containing the suspensions were rapidly plunge-frozen in liquid nitrogen. The holders containing the samples were then mounted onto a Denton complementary freeze-etch specimen cap that was used to fracture the samples by lifting and rotating the fracture arm of the cap by 180 degrees. A standard flat holder containing the specimens was attached to the cryo-transfer arm and inserted into the prechamber of an Oxford CT 1500 Cryotrans System mounted on a Hitachi S-4000 field emission scanning electron microscope to perform low-temperature manipulations and observations. The specimens were either sputter-coated with platinum in the prechamber and inserted onto the cryostage of the microscope or etched and coated in the prechamber and moved to the cryostage for observation. Accelerating voltages of 10 kV were used to observe and record images onto Polaroid Type 55 P/N film.

Results

Line drawings of major anatomical regions of the adult stage of male and female specimens of *Pratylenchus penetrans* are shown in Figure 1. The anterior region of the lesion nematode is characterized by a robust stylet (Fig. 2) supported by extensive protractor muscles that extend from the cephalic framework and body wall to the stylet basal knobs with lateral contact to the stomatal wall (Figs. 1–5). The lip region shows a distinct boundary with the body cuticle delineating a sharp depression (Figs. 4, 5) between annules 3 and 4. The anterior sensory organs of nematodes consist of circular arrangements of sensilla arranged in a hexaradiate pattern and comprised of 6 inner labial, 6 outer la-

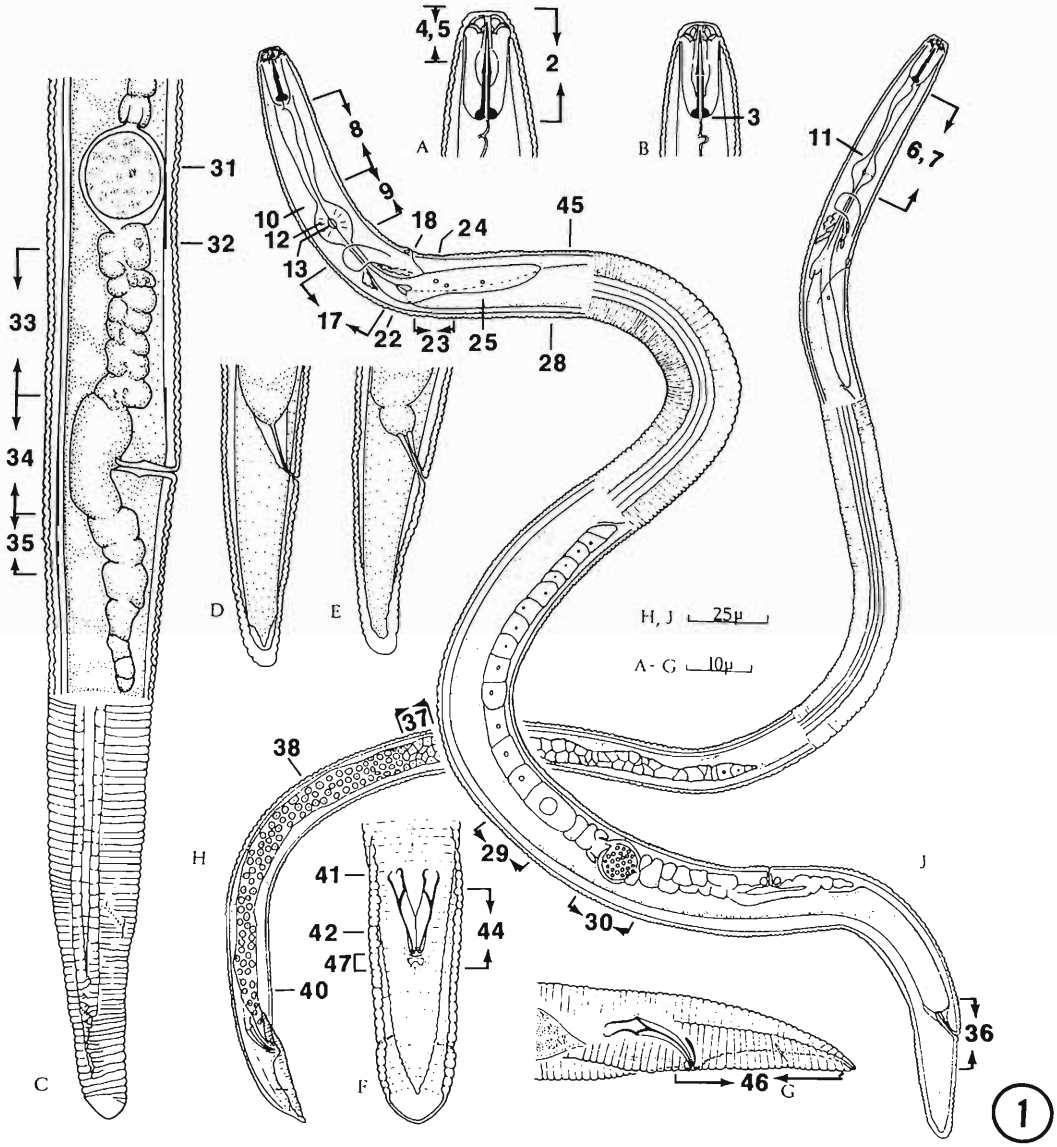

Figure 1. ***Pratylenchus penetrans*. A. Female head. B. Male head. C. Female vulva region and tail. D, E. Female tail tips. F, G. Male tails in ventral view (F) and lateral view (G). H. Male. J. Female. (A–G, topotypes, courtesy M. W. Allen). Reprinted with permission from D. C. M. Corbett. 1973. C.I.H. Descriptions of Plant-Parasitic Nematodes, Set 2, No. 25, © Commonwealth Agricultural Bureaux. Numbers indicate the approximate locations of figures used to describe various anatomical regions of *P. penetrans*.**

bial, and 4 cephalic sensilla. The amphidial receptors consist of 7 cilia that extend anteriad through the amphidial canal.

The esophageal lumen extends from the stylet base as a tubular system to the triradiate pump lumen (Fig. 1). It then continues as a triradiate cuticularized canal to the esophago-intestinal valve consisting of appressed unlined membranes of a pair of enlarged cells. The cuticularized lumen wall of the esophagus branches just posteriad to the stylet knobs, and the dorsal branch terminates as a quadriradiate valve shown obliquely in the dorsal gland ampulla (Fig. 6). The dorsal gland ampulla and the

slightly narrow elongated dorsal gland extension of the procorpus is filled with small, electron-opaque granules (Figs. 6, 7). The ampulla and adjoining dorsal gland extension follow a sinuous pathway through the procorpus adjacent to the lumen of the esophagus (Figs. 6, 7). In contrast to the dorsal gland extension shown in Figures 6 and 7, the dorsal gland extension in Figure 8 is greatly expanded and filled with numerous secretory granules exhibiting various electron densities and occupying a major part of the procorpus (Figs. 8, 9). Differentiation of a distinct dorsal gland ampulla is absent.

As the dorsal gland extension traverses the anterior region of the metacorpus, the extension appears constricted. It is surrounded by sphincter muscles (Fig. 10) that probably control the anterior flow and accumulation of secretory granules (Fig. 9) originating in the dorsal gland. Slightly posteriad to the sphincter muscles are parallel arrays of membranes associated with anterior muscles of the metacorpus (Fig. 11). At the midregion of the metacorpus, the walls become thickened and form the triradiate valve of the metacorpus pump (Figs. 12, 13). Hexaradiate bands of muscles are connected by hemidesmosomes to adradial positions of the triradiate valve wall (Fig. 13). Muscle elements extend centrifugally and longitudinally to the basal lamellae of the metacorpus where they are anchored. The triradiate appearance of the lumen wall of the central metacorpus is indicative of the relaxed state of the pump muscles. Contraction of these muscles would open the valve and allow passage of food from the stylet to the posteriad region of the esophagus and the intestine. Slightly posteriad from the central metacorpus pump valve, the cuticle lumen wall branches twice ventrally and posteriad to form cuticular tubes (Figs. 14–16) that terminate as quadriradiate valves within ampullae of subventral glands. The triradiate metacorpus valve lies parallel and central to the dorsal and subventral gland extensions that continue through the metacorpus sphincter muscles (not illustrated). The isthmus of the esophagus is enclosed by the nerve ring (Figs. 17, 18). The nerve processes forming the lateroventral commissure originate at the base of the nerve ring, slightly anterior to the level of the outlet of the secretory-excretory gland (Figs. 17, 19). In longitudinal view, the esophago-intestinal valve is preceded by the triradiate lumen of the esophagus surrounded by supporting membranes and terminating as a large cavity surrounded by epithelial cells of the intestine (Figs. 20, 21). The valve consists of 2 large nucleated cells. The lumen aperture forms by separation of adjacent nonlined membranes of the cells (Figs. 21, 22). Lateral membrane junctions limit loss of lumen contents. The dorsal gland extension widens abruptly posteriad from the isthmus to become part of the gland body (Figs. 23, 24). The esophago-intestinal valve and the dorsal gland nucleus lie in about

→

Figures 2, 3. Sections through stylet region of *Pratylenchus penetrans*. 2. Longitudinal tangential view of a retracted stylet (St). Protractor muscles (Pm) extend from the base and anterior surfaces of the stylet knobs to attachment sites at the stomatal wall (SW), cephalic framework (CF), and lateral body somatic muscle elements. Sk, stylet knob. 3. Cross-section slightly below stylet knobs shows electron-opaque accumulations (EDA) associated with electron-lucent filaments that are continuous with the main protractor muscle elements. Portions of the amphidial gland sensilla (Se) and a pair of microvillus nerve processes (NP) are also apparent. EL, esophageal lumen. Scale bars = 1.0 μm.

Figures 4, 5. Oblique sections through stoma and cephalic regions of an adult male *P. penetrans*. 4. Stomatal cavity in relation to body cuticle (cu), cephalic framework (CF), and anterior sensilla (Se). ACC, amphidial cuticular channel; Pm, protractor muscle; sc, stomatal cuticle; Sm, somatic muscle. 5. Section through blades (CFB) of cephalic framework and thick region of the stomatal wall (SW) shows portions of the amphidial sensilla (ASe), cephalic receptors (CR), and accessory receptors (AR). Pm, protractor muscles; Sm, somatic muscles; St, stylet. Scale bars = 1.0 μm.

Figures 6, 7. Longitudinal sections through procorpus and metacorpus of *P. penetrans*. 6. Dorsal gland extension (Dx) and ampulla (DA) containing small secretory granules (SG) lie medially in anterior region of the procorpus. Numerous mitochondria (Mc) extend posteriad from the base of the stylet knobs shown in Figure 2 to the supporting cells of the procorpus. 7. Section posteriad to that shown in Figure 6. Transversely oriented dorsal gland extension (Dx) is folded and contains strongly to moderate electron-opaque granules. The dorsal gland extension and adjacent tubular cuticularized wall (EL) of the esophageal lumen enter the metacorpus (m) shown in a submedial tangential section. Scale bars = 1.0 μm.

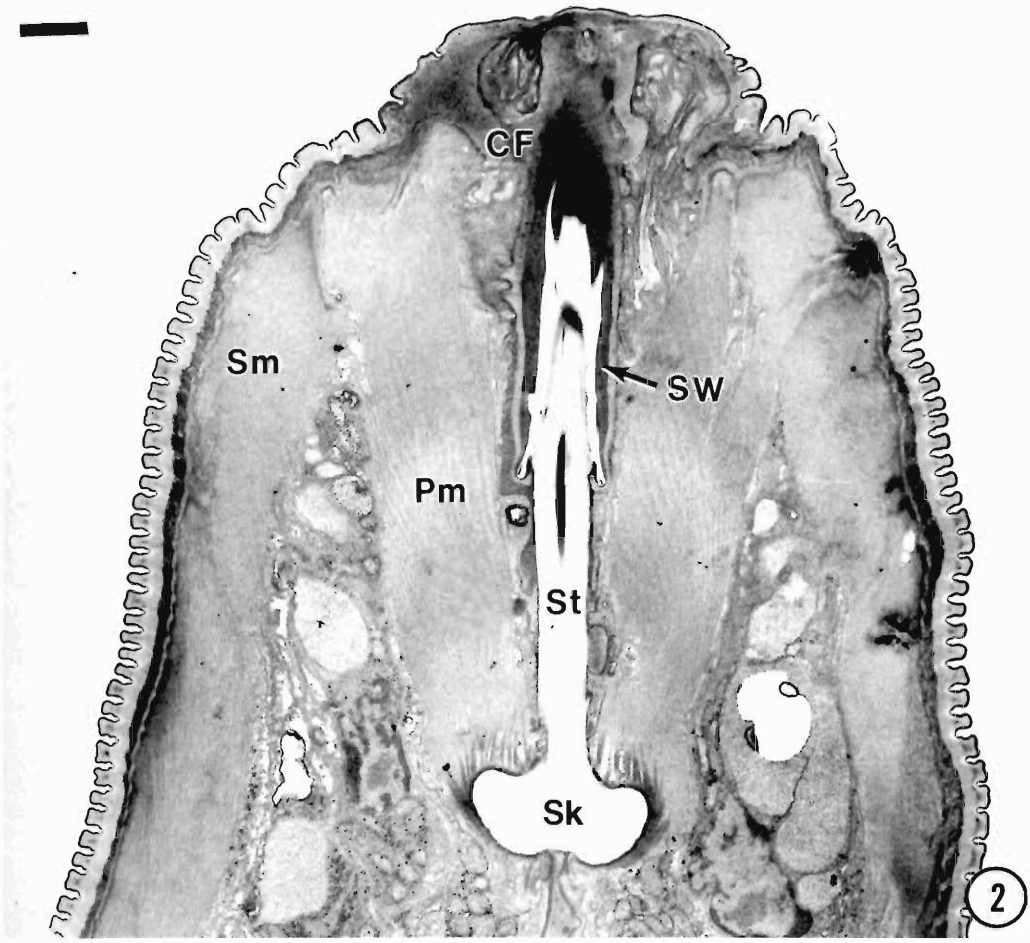

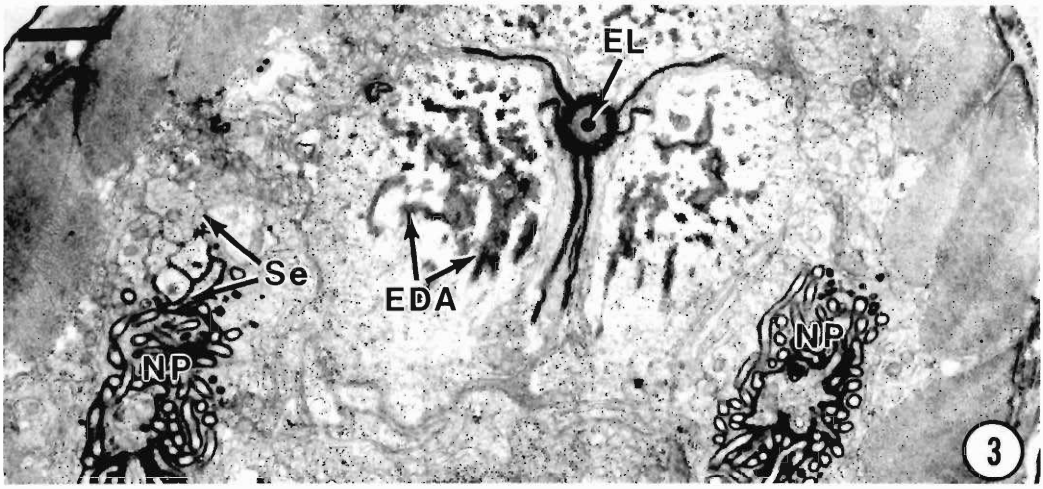

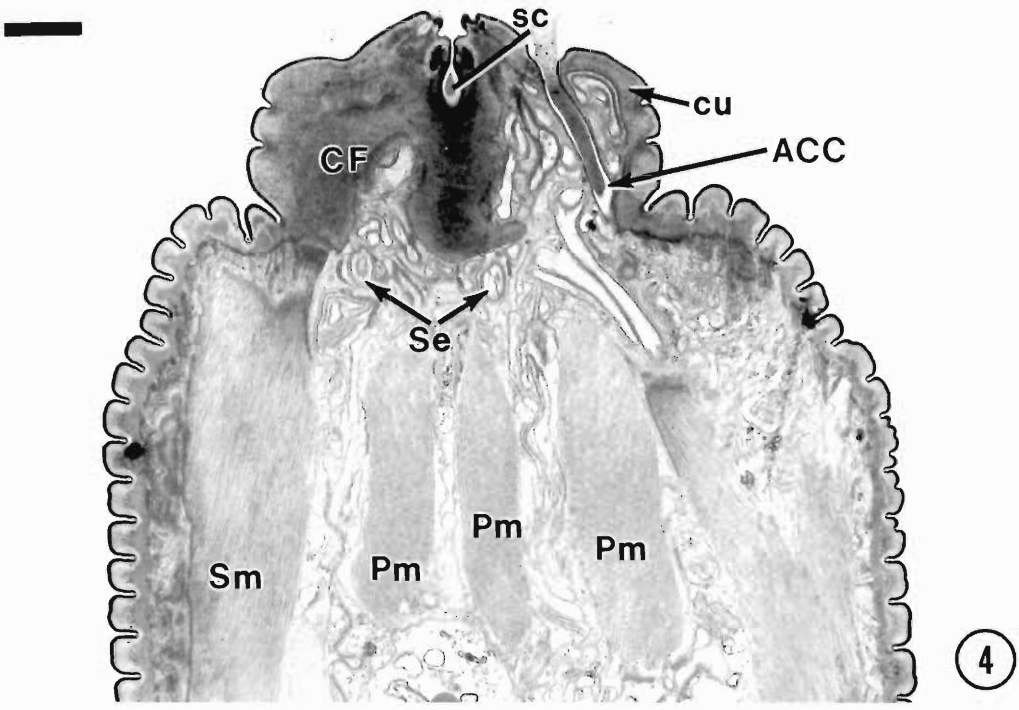

4

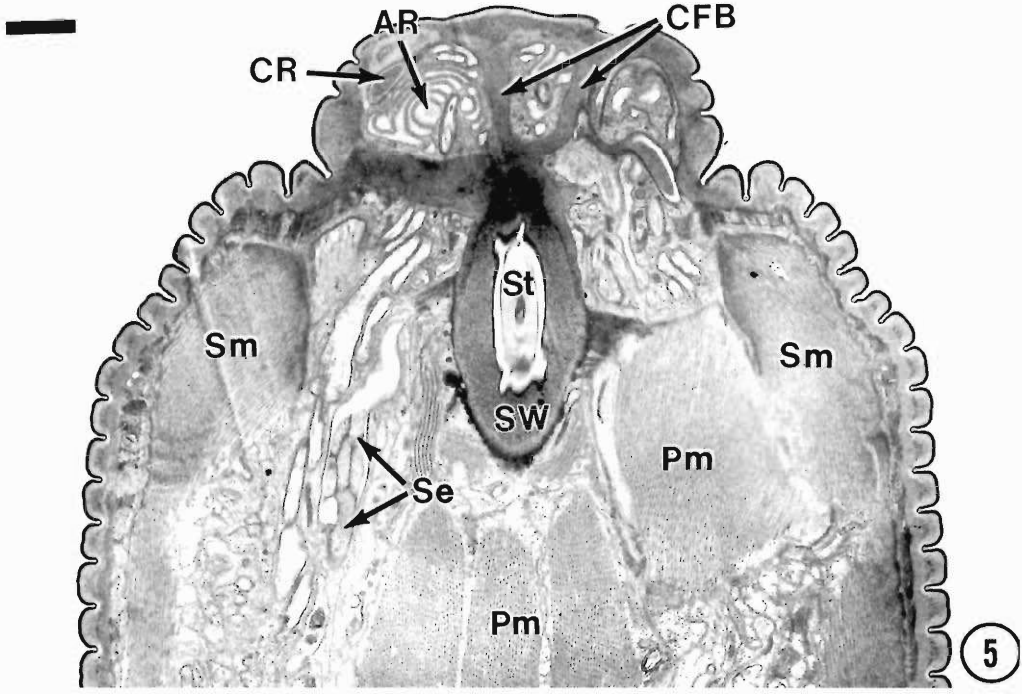

5

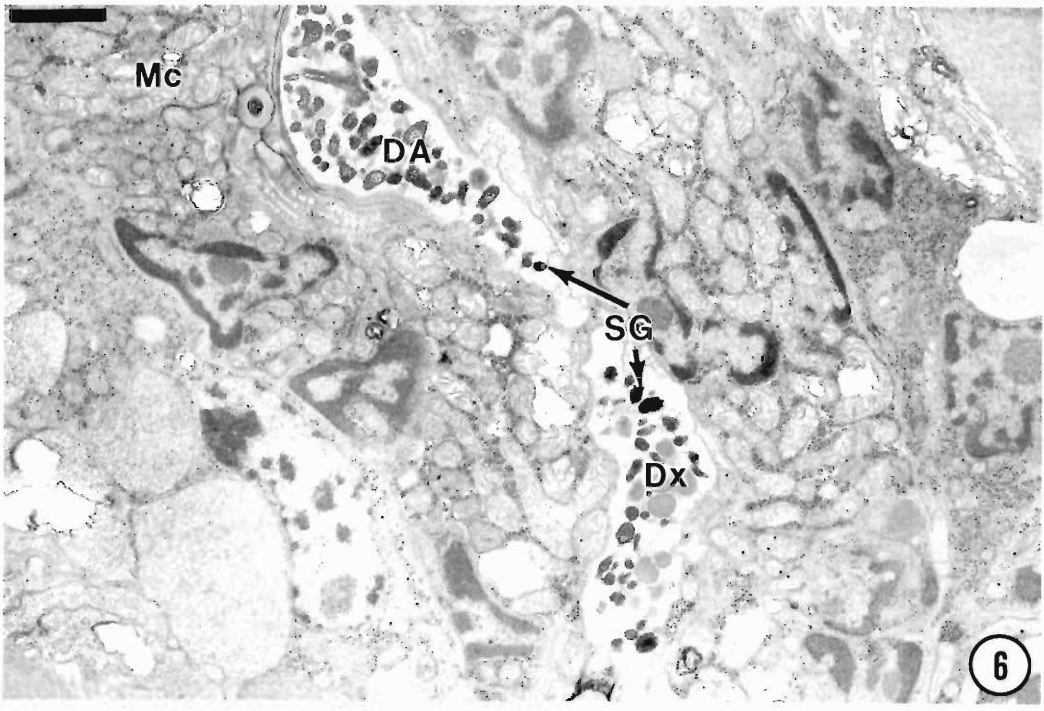

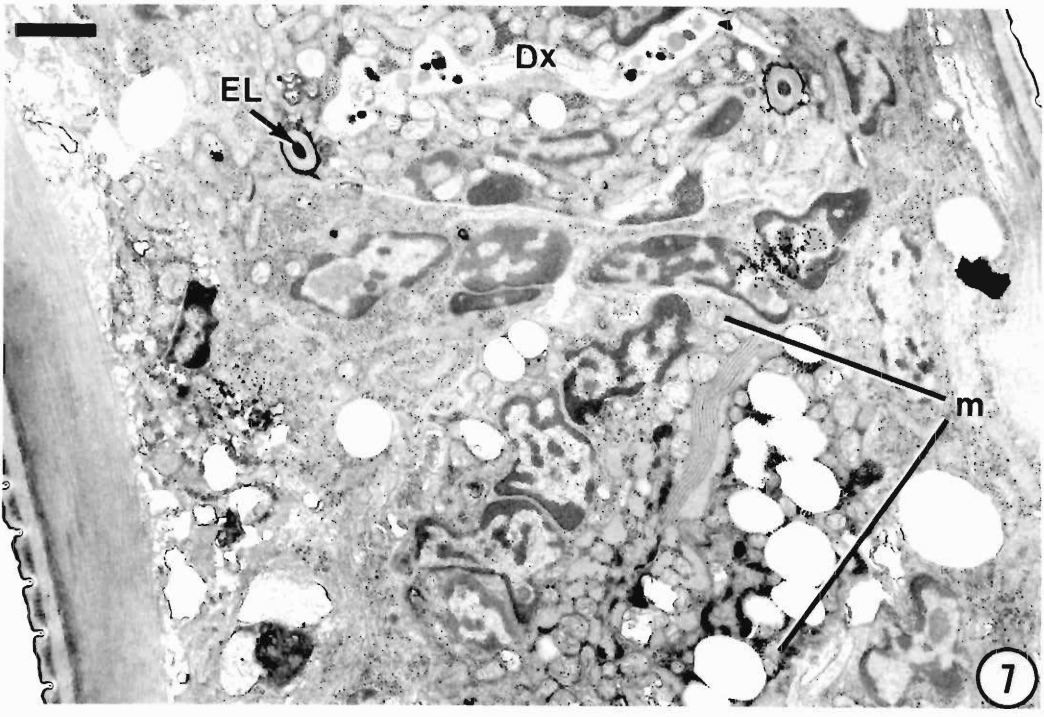

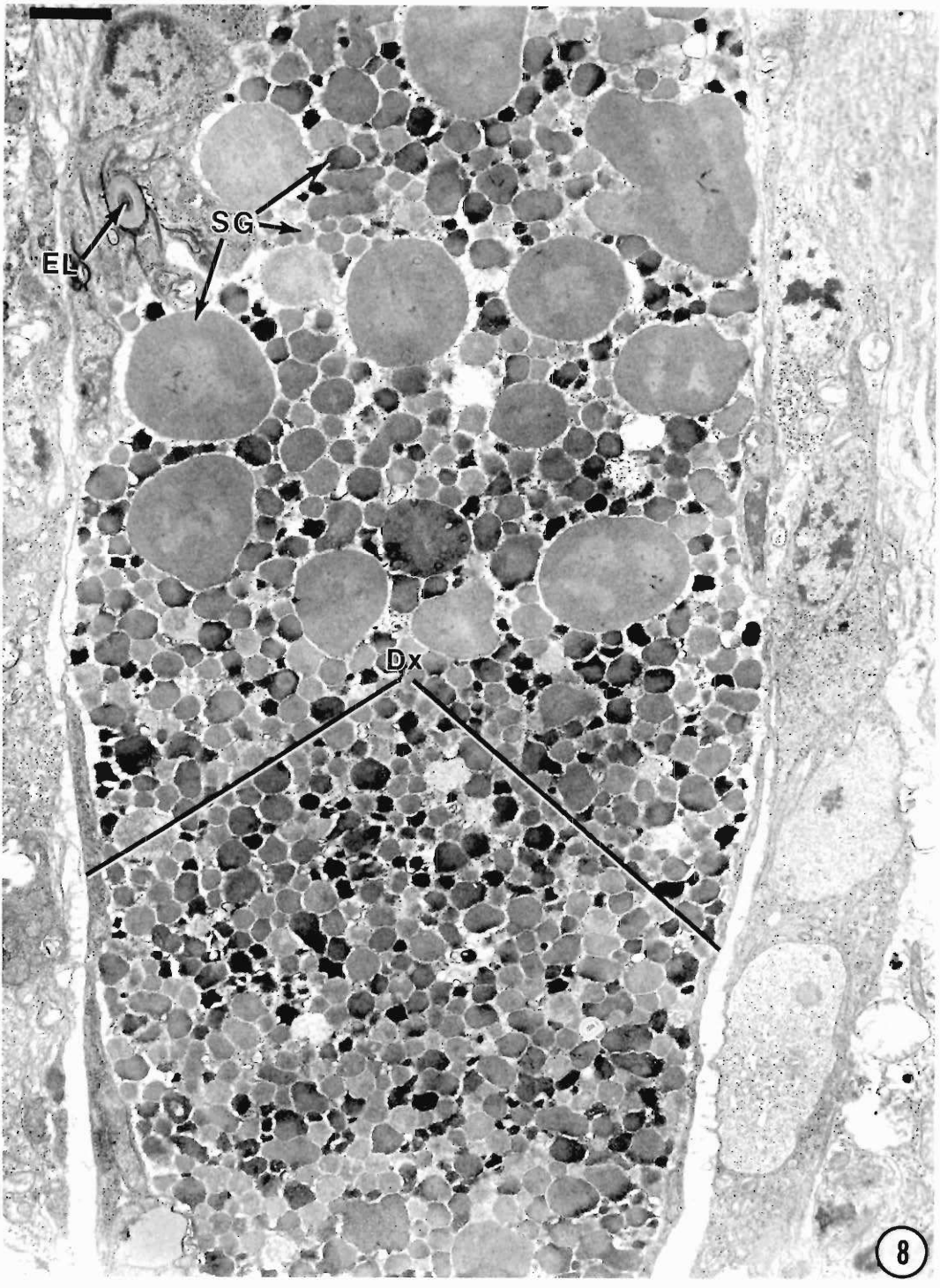

Figure 8. Longitudinal section of adult female of *P. penetrans* showing expanded dorsal gland extension (Dx) within the procorpus of the esophagus. Secretory granules (SG) are small to large in size and light to moderate in electron density. EL, esophageal lumen. Scale bar = 1.0 μm.

the same cross-sectional plane (Fig. 22). Within the dorsal gland, small electron-opaque secretory granules are assembled by Golgi complexes. The secretory granules appear as electron-opaque clusters of condensation products in various stages of enlargement and dissipation (Fig. 23). The prominent dorsal gland nucleus is surrounded by Golgi complexes and their secretory products (Fig. 24).

The subventral glands (Figs. 25, 26), which are adjacent and posteriad to the dorsal gland, terminate in a narrow region between the intestinal epithelium, the ventral nerve cord, and the somatic musculature. The subventral gland nuclei, which tend to be smaller than the dorsal gland nucleus, frequently have convoluted membranes (Fig. 26). Golgi complexes surround the nuclei and give rise to electron-opaque secretory granules that form smaller, less compact clusters than those observed in dorsal glands (Figs. 25, 26).

The secretory-excretory gland terminus is a tubular invagination of the body cuticle (Fig. 19) that extends into the elongated gland. The central lumen of the secretory-excretory gland is delineated by an electron-opaque wall that is surrounded by membranous vesicles and tubules (Fig. 20). The secretory-excretory gland body extends posteriad between the borders of the esophageal glands and intestinal epithelium.

The intestinal lumen occasionally appears occluded with a membrane complex (Fig. 27), especially when the body space is shared with reproductive organs that compress the intestines. However, in the region beyond the esophagointestinal valve, the lumen is broad and clear of ingested materials (Figs. 20, 21). In regions where the intestinal lumen is filled with contents, the lumen wall is greatly distended (Fig. 28). The filamentous or vesicular membranous invaginations along the inner wall of the lumen appear to be sections through widely dispersed intestinal microvilli. The intestinal lumen is formed by paired epithelial cells that are joined laterally by membrane junctions (Fig. 28).

Adjacent and parallel to the intestine is the ovary or testis. Beyond the germinal zone of the ovary, primary and secondary oocytes are formed. Enlarged oocytes (Fig. 29) can pass through the oviduct (Fig. 29) into a spermatheca (Figs. 1, 30). The spermatozoa within the spermatheca (Fig. 30) are similar in morphology to

---

→

Figure 9. Section through the metacorpus of adult female of *P. penetrans* with an oblique view of the triradiate lumen of a sclerotized valve (v) of metacorpus (m) and parts of the dorsal (Dx) and subventral gland extensions. Secretory granules in the dorsal gland extension within the metacorpus appear uniformly small compared to the wide range of sizes that are found in the gland extension of the procorpus of the specimen in Figure 8. Secretory granules in the subventral gland ampullae (SvA) are also small and moderately electron-dense. nr, nerve ring. Scale bar = 1.0 μm.

Figures 10, 11. Cross-sections through the anterior regions of the metacorpus of *P. penetrans*. 10. Adult male sphincter muscles (Spm) surround a narrow region of the dorsal gland extension (Dx) containing a few secretory granules and closely assembled microtubules (Mt). EL, esophageal lumen. 11. Section posteriad from the sphincter near the main body of the metacorpus. Laminar membrane (LM) complexes are associated with the muscle system of the anterior metacorpus. Dx, dorsal gland extension; EL, esophageal lumen; N, nucleus. Scale bars = 1.0 μm.

Figures 12, 13. Median cross-sections of metacorpus in *P. penetrans* show protractor muscle in relation to the esophageal pump valve and supporting basal lamina. 12. Cuticle of the esophageal lumen (EL) showing transition from circular to modified triradiate shape of the lumen wall. Dx, dorsal gland extension; mm, metacorpus muscles. 13. Metacorpus valve (mv) with triradiate thick sclerotized walls of the lumen. Metacorpus pump muscles (mpm) are attached centripetally to adradial walls of the valve and centrifugally to the metacorpus wall via hemidesmosomes (hd). cuR, cuticular ridges; Dx, dorsal gland extension. Scale bars = 1.0 μm.

Figures 14–16. Cross-sections showing dorsal gland extension (Dx) and components of subventral gland valve of *P. penetrans*. 14. Expanded lumen of esophagus (EL) shows one lateral wall with opening into cuticularized base (→) of a subventral gland valve (Svv). mpm, metacorpus pump muscle. 15. Closed triradiate esophageal lumen (EL) flanked subventrally by cuticular bases (cb) of valves leading to subventral gland ampullae. Dx, dorsal gland extension. 16. Quadriradiate-shaped membrane terminals of subventral valves (Svv) posteriad from region illustrated in Figure 15. Dx, dorsal gland extension. Scale bars = 1.0 μm.

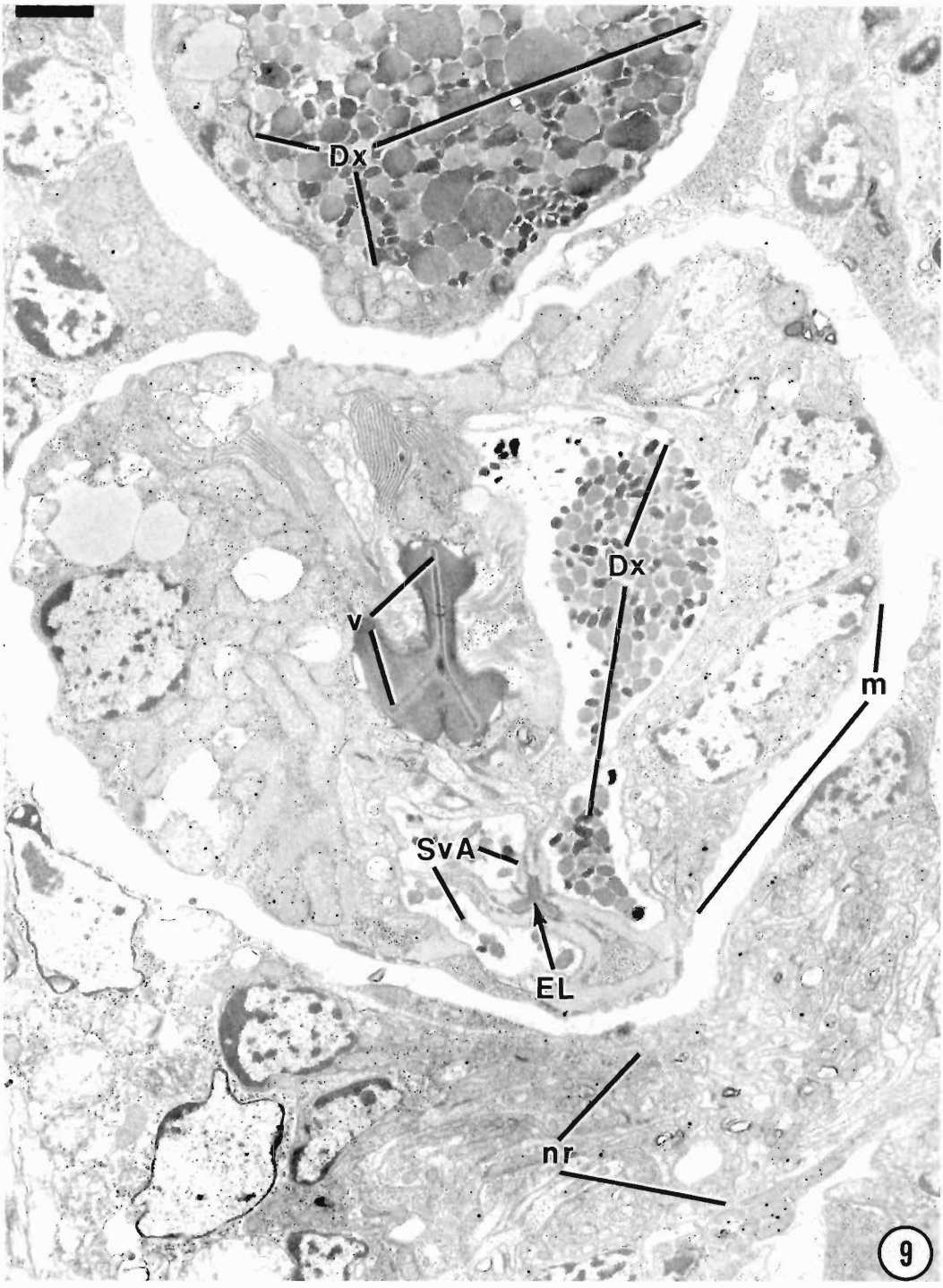

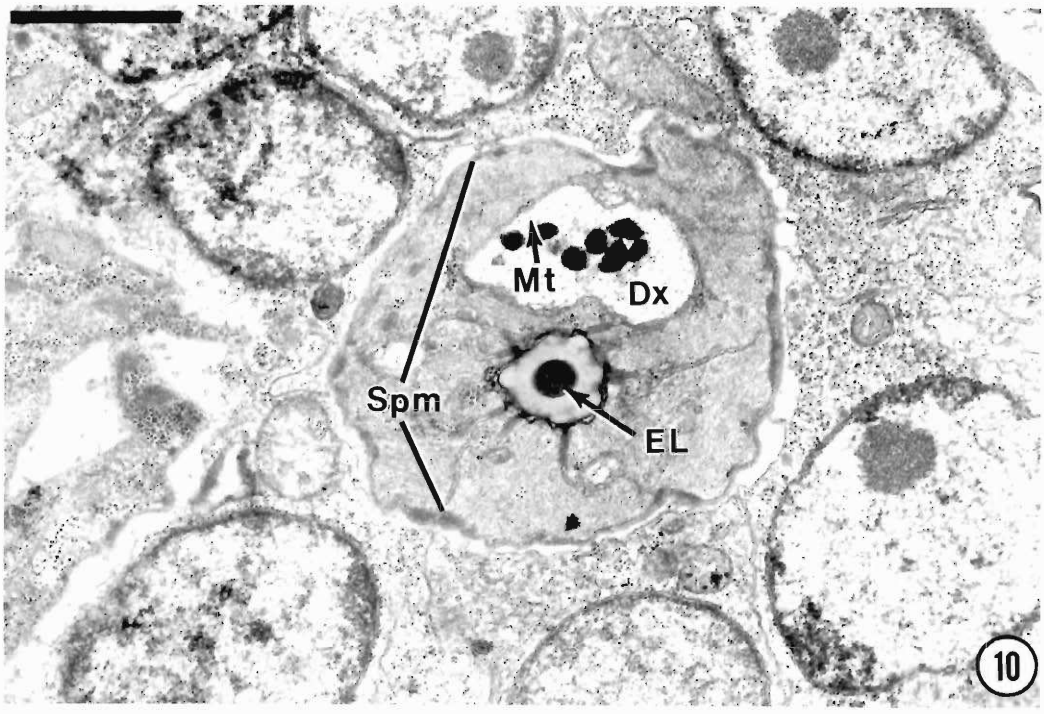

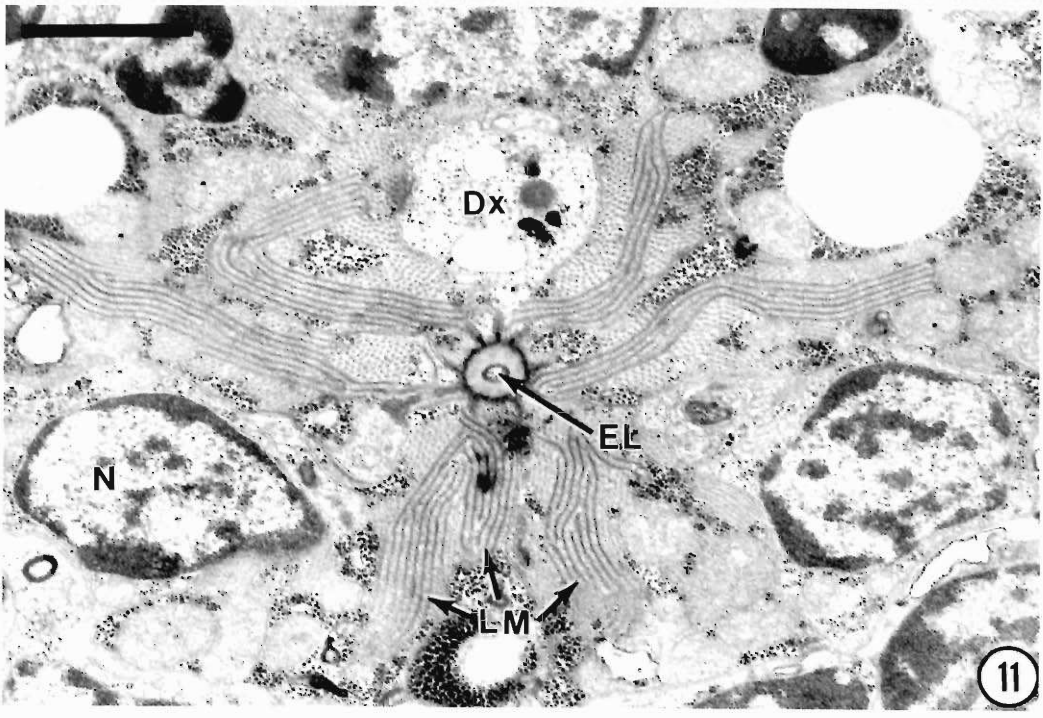

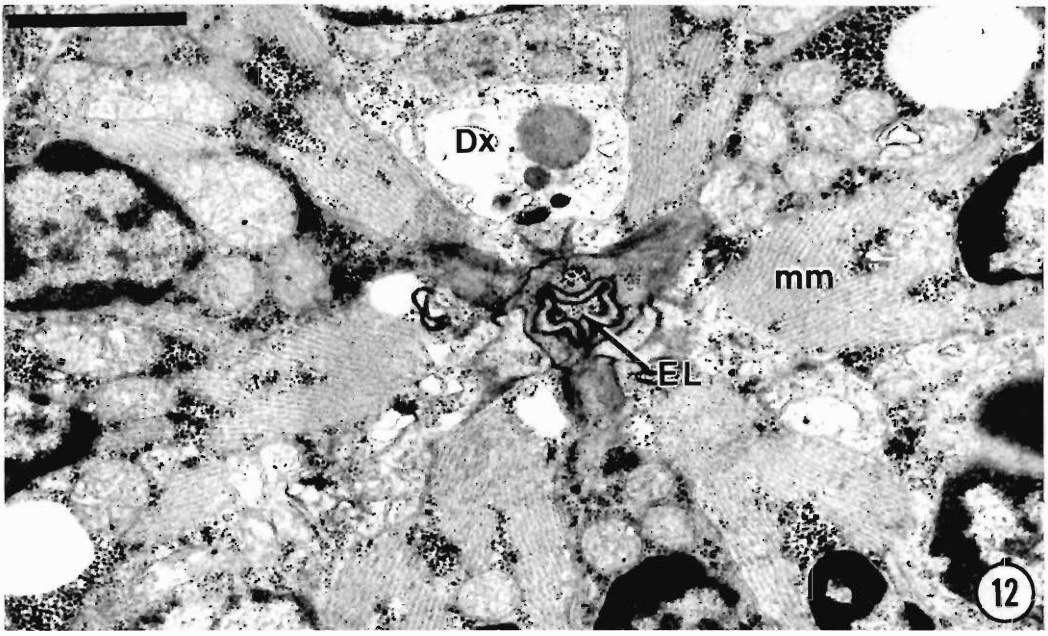

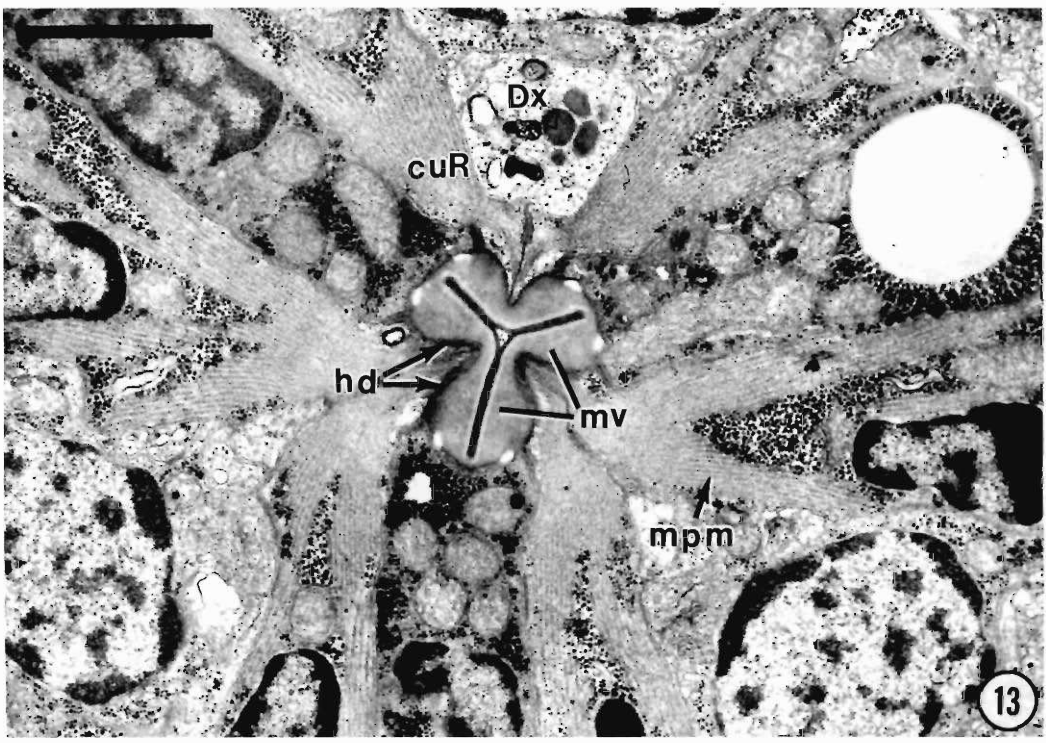

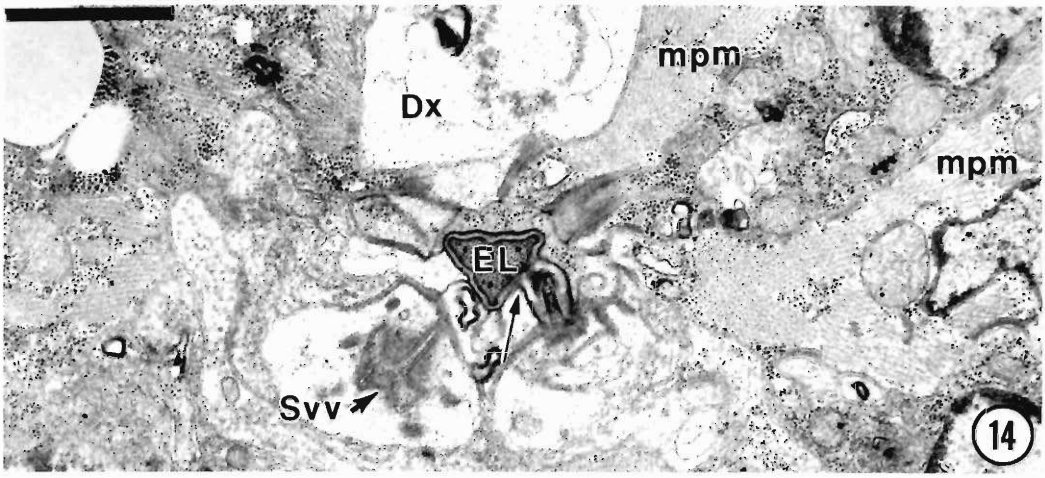

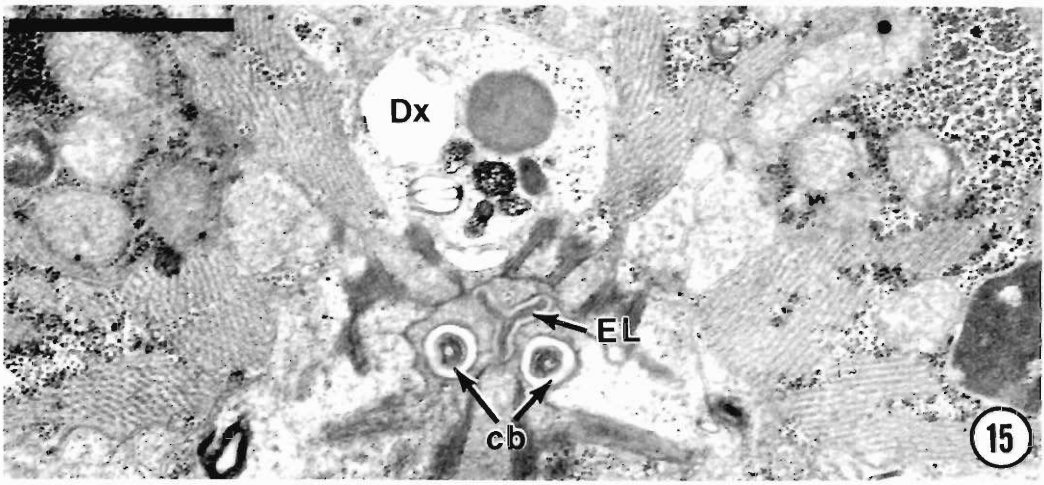

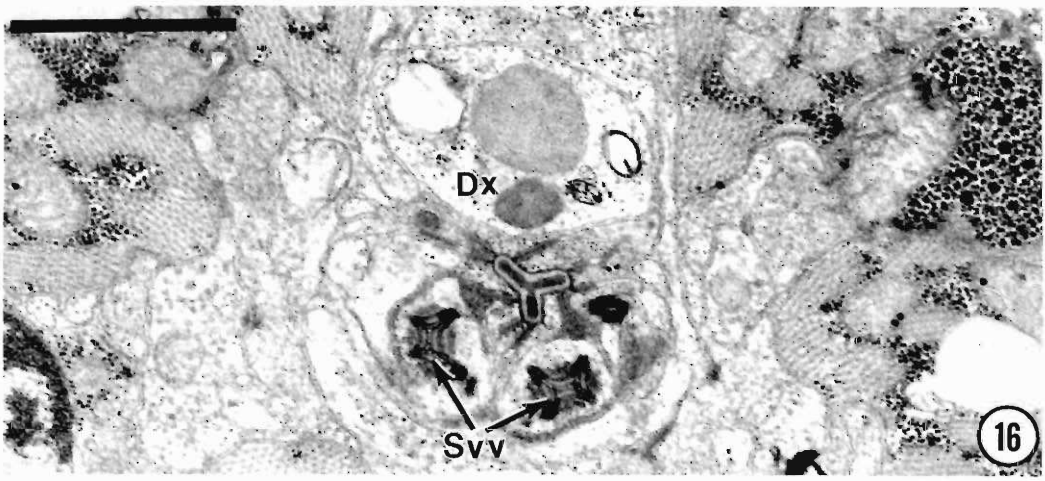

Figure 17. Longitudinal section through the isthmus (i) of the esophagus of adult male of *P. penetrans*. The nerve ring (nr) is located close to the metacorpus base and lies anteriad the base of the esophago-intestinal valve. A ventrolateral commissure of nerve fibers appears between the somatic muscles and the cuticle to form the hemizonid (hz). The hemizonid is located ventrolaterally midway between the base of the nerve ring and esophago-intestinal valve. Scale bar = 1.0 μm.

sperm observed in the vas deferens of a male specimen (Fig. 1). Each spermatozoon has irregular masses of chromatin consisting of nuclear material not bounded by a nuclear envelope, mitochondria, and small clusters of fibrous bodies (Figs. 30, 40). Fertilization occurs in the spermatheca where numerous sperm accumulate. In *P. penetrans*, stain reactions were not available to show this sequence of events. An oocyte within the spermatheca region of the uterus (Fig. 31) is filled with electron-transparent lipid granules and electron-opaque protein bodies and bounded by a unit membrane with regions of electron-opaque deposits. Columnar cells extend from the spermatheca to the fluid-filled region opposite the vaginal canal (Figs. 30, 32, 33). These cells are characterized by a dense concentration of ribosomes, mitochondria, and Golgi complexes and their secretory granules of various sizes and shapes. The cells have a centrip-

etal orientation; their bases are joined by membrane junctions. A central lumen, which is lined with the apices of these cells, provides the passage for eggs and spermatozoa (Fig. 32). The basal membranes of the columnar cells, which are highly plicated, apparently allow for expansion of the lumen during egg passage (Figs. 30, 32, 33). The lumen of this region of the uterus is readily identified by the electron-opaque membrane junctions that connect the basal portions of adjacent cells (Fig. 32). The lumen of the columnar region is continuous with the fluid-filled uterus that opens into the cuticle-lined vagina (Fig. 34). A postvulval uterine sac occurs posteriad to the central uterus (Fig. 35). In longitudinal section, the vaginal cuticle forms a flat contoured channel that initially appears convoluted near the vulva and is continuous with the body cuticle (Fig. 34). A group of muscles is attached by hemidesmosomes to the flat region of the vaginal cuticle in lateral view. Muscle filaments are primarily tangential, but some horizontal orientations also occur. Two pairs of striated muscles with longitudinal to tangential orientations are attached by hemidesmosomes to the anterior and posterior cuticle walls of the vulva. The conformation and position of the muscles, which lie adjacent to the vaginal canal and the walls of the vulva, appear to have a direct relationship with the egg-laying process. The rectum and the anus are located subterminally (Fig. 36).

The male gonad consists of a single testis and vas deferens. The germinal zone of the testis gives rise to spermatogonial cells that develop into primary and secondary spermatocytes. The transition from spermatocytes to spermatids involves the reduction division of chromosomes from diploid to haploid within a short region of the testis. During this transition, the nuclear membrane of the spermatocyte (Fig. 37) disappears. After meiosis, the haploid chromosome complement appears as electron-opaque chromatin within an amoeboid cell (Fig. 38). Spermatid cell membranes evaginate to form filopodia that interdigitate with boundaries of adjacent spermatids to form distinctive membrane complexes. Large clusters of fibrous bodies surround the central nucleus and later become dispersed throughout the cytoplasm (Figs. 38, 39). Some fibrous bodies persist in the spermatozoa as shown in a section through a spermatheca (Fig. 30). Nuclei of spermatozoa, which tend to be irregular, are surrounded by clusters of mitochondria (Figs. 30, 40). The nonnuclear regions of the sperm are generally electron-translucent; they frequently have remnants of fibrous bodies similar to those occurring in spermatids. As sperm become concentrated in the vas deferens, their outer boundaries become ovoid to elliptical. Their membrane surfaces form pseudopodia or evaginate into filopodia that appear as tubules or small vesicles (Fig. 40).

The ultrastructure of the male copulatory organs of *P. penetrans* has been described in detail by Wen and Chen (1976). Additional micrographs of the spicules and their related structures are shown as a corollary to other organs described in this paper. The base of the spicule shaft is supported by protractor and retractor muscles (Figs. 41, 42). The elongated arms of the spicules (Figs. 42–44) extend downward and centrad to enter the cloaca (Fig. 44). A pair of sensilla is located at the posterior lip of the clo-

→

Figures 18–20. Sections through the isthmus and secretory-excretory gland of *P. penetrans*. 18. Triradiate wall of esophagus. Membrane junctions (MJ) interact with limiting membranes of dorsal (Dx) and subventral gland extensions (Svx). The section includes a part of the nerve ring (nr). 19. A cross-section of an adult male posteriad from the nerve ring shows narrow region of esophagus (E) and the cuticle-lined duct (SED) of the secretory-excretory gland. Svx, subventral gland extension. 20. Longitudinal section of an adult male shows a portion of the cuticle-lined duct within the secretory-excretory canal (SEc). Vesiculate membranes (VeM) occur in the space between the duct wall and the limiting membrane of the secretory-excretory gland. IE, intestinal epithelium; IL, intestinal lumen. Scale bars = 1.0 μm.

Figures 21, 22. Sections through esophago-intestinal regions of *P. penetrans*. 21. Longitudinal section of the esophago-intestinal valve of an adult male with a membrane supported terminus of cuticle-lined esophageal lumen (EL) and continuity with unlined nonmuscular cells comprising the esophago-intestinal valve (Eiv). The posterior boundary of the valve adjoins or leads into an enlarged vacuolate intestinal lumen (IL). 22. Cross-section of esophago-intestinal valve (Eiv) is shown adjacent to the expanded region of the dorsal esophageal gland (Dg). Scale bars = 1.0 μm.

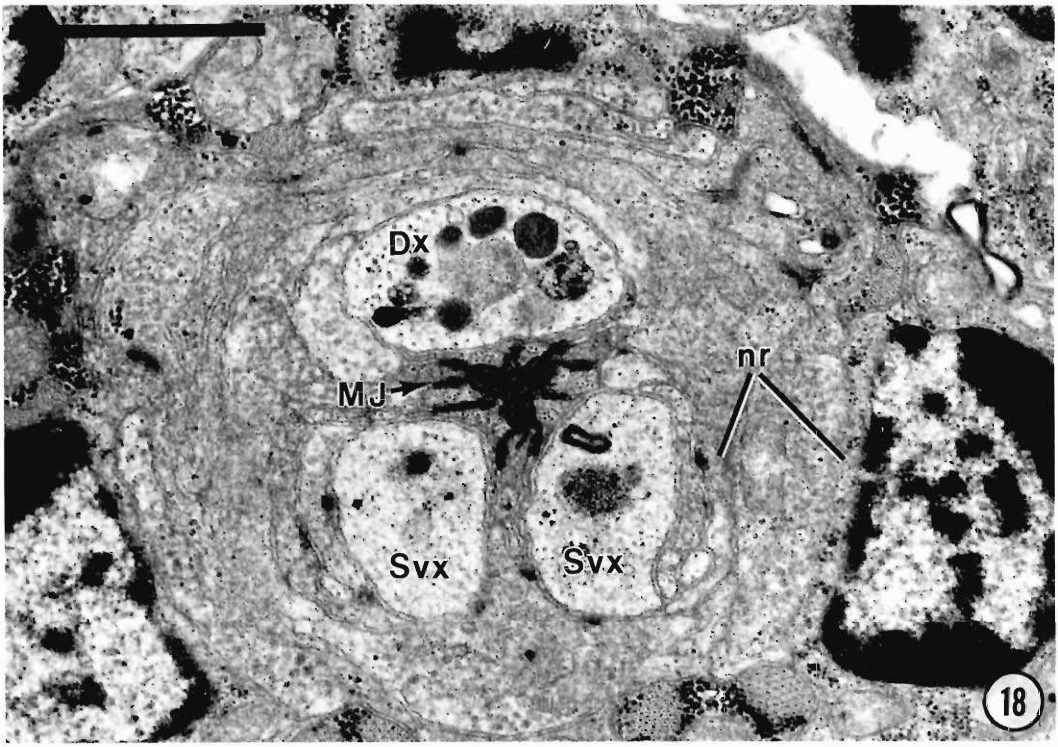

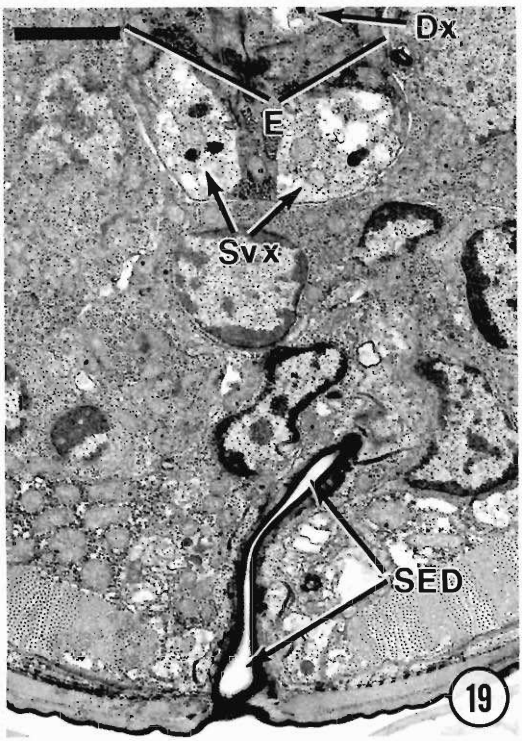

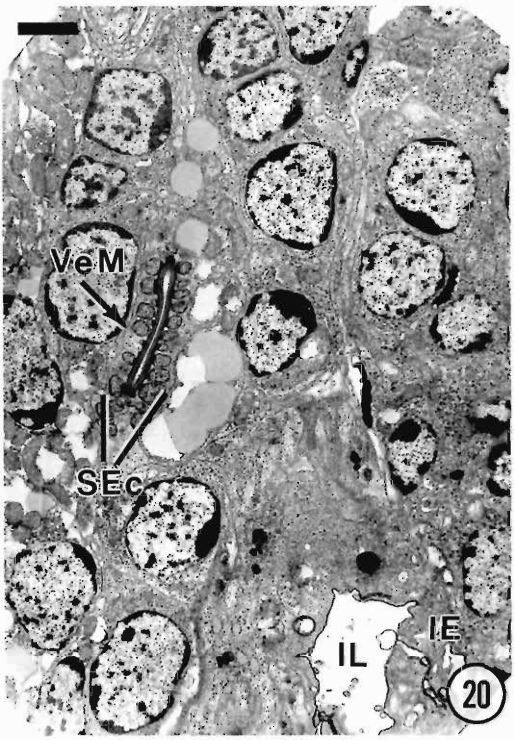

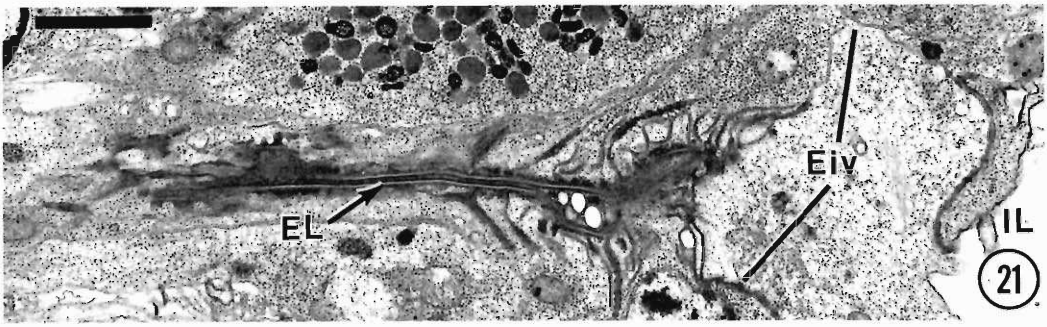

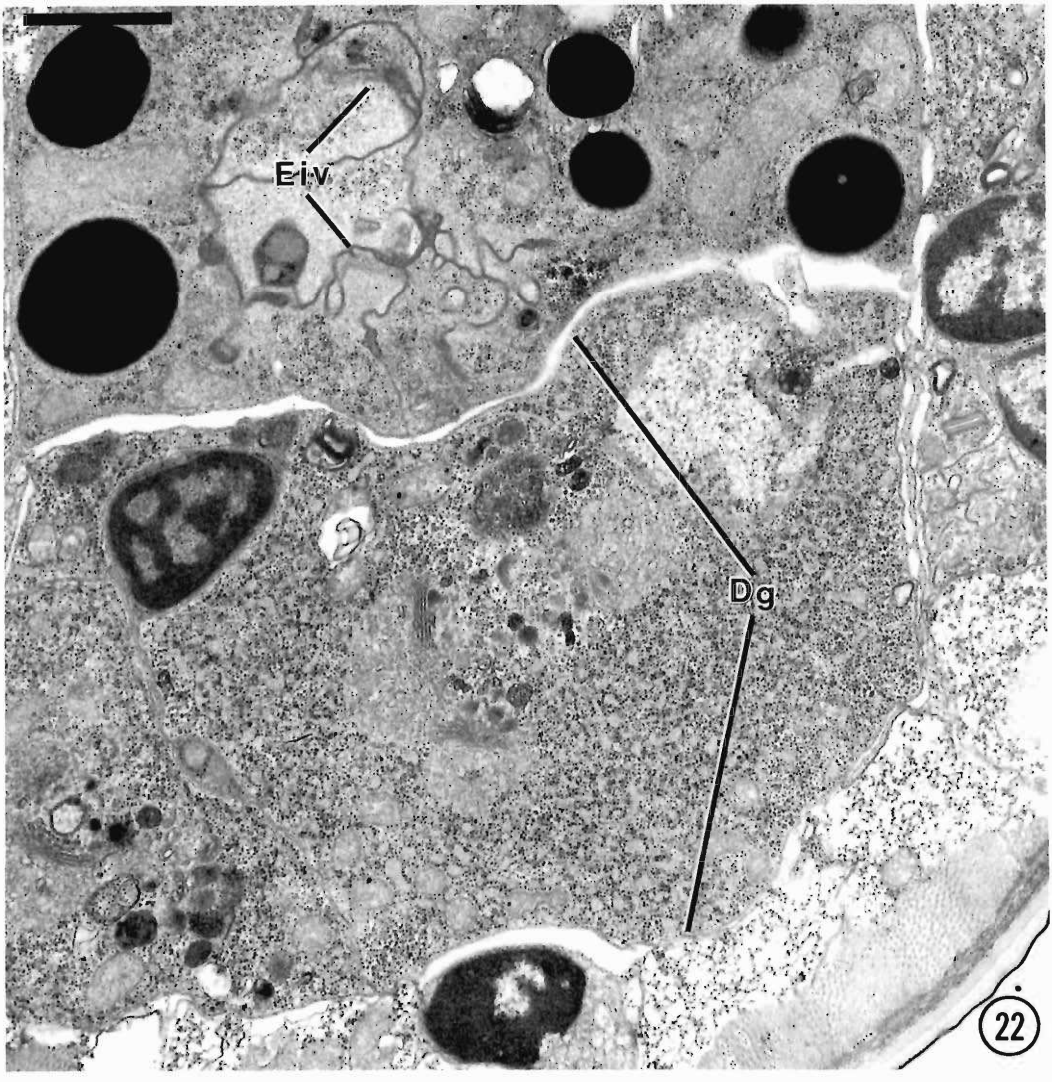

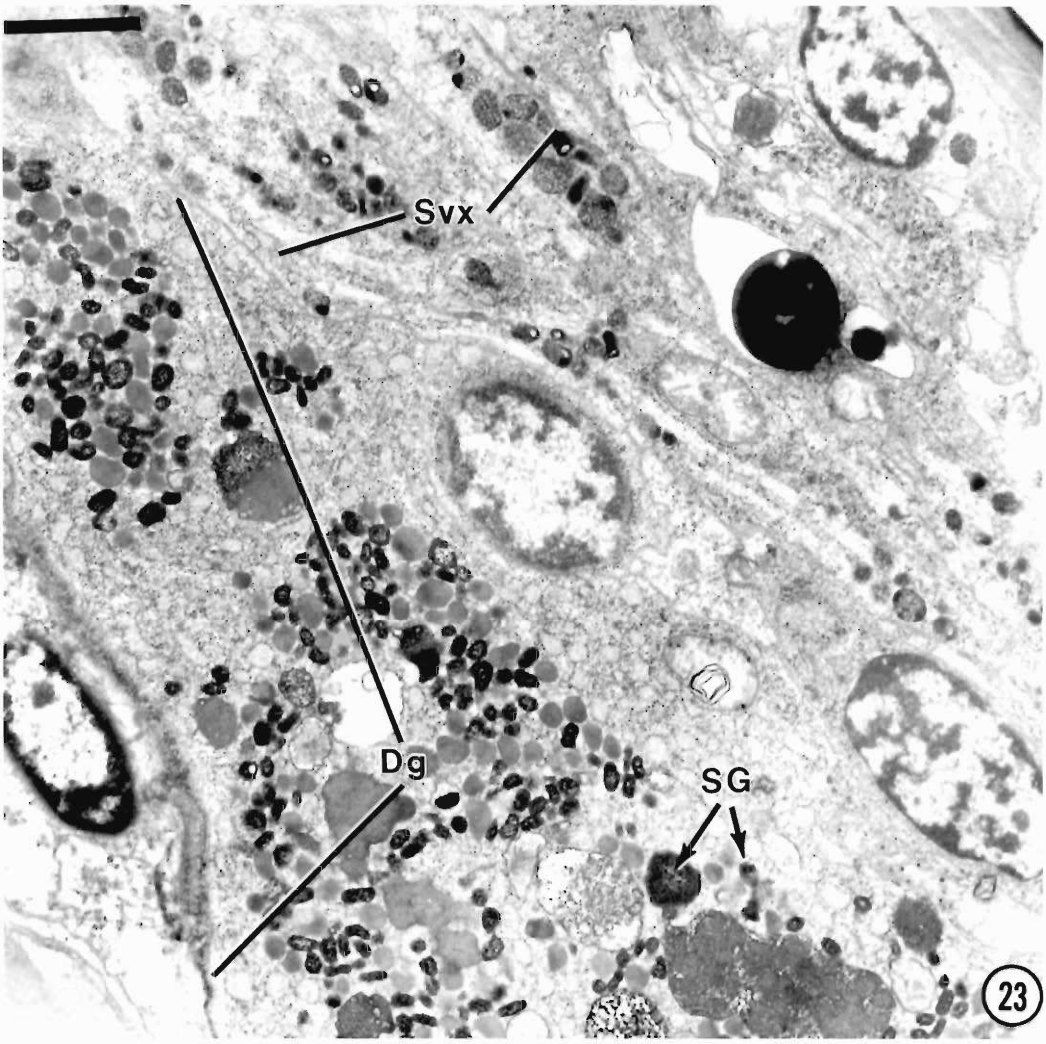

Figure 23. Longitudinal section of anterior region of the dorsal gland (Dg) of adult male of *P. penetrans*. Cytoplasm filled with dense clusters of electron-opaque secretory granules (SG) that appear to condense into larger granules. Svx, subventral gland extension. Scale bar = 1.0 μm.

aca (Fig. 44). Copulatory caudal alae extend from the cloaca to the tail terminus (Fig. 46).

Low-temperature cryofixation and scanning electron microscopy of specimens helps to verify structure–function relationships. Freeze-fractured images of the intestinal region (Fig. 45) corroborate the presence of the large lumen of the central region of the intestine as observed by transmission electron microscopy of glutaraldehyde-fixed specimens (Fig. 28). Within the lumen of the intestine, microvilli-like membrane invaginations are prominent but lack the uniform microvilli arrangement observed in other species. In addition to the membrane invaginations of the lumen wall, a few evaginations appear to extend into the intestinal epithelial cells. However, these evaginations could result from the slightly folded boundaries of the lumen. The secretory-excretory gland duct appears tubular in the anterior region of the gland cell. In chemically fixed specimens, the duct walls usually appear collapsed (Fig. 26). However, with the cryofixed specimens observed with LTSEM, the secretory-excretory

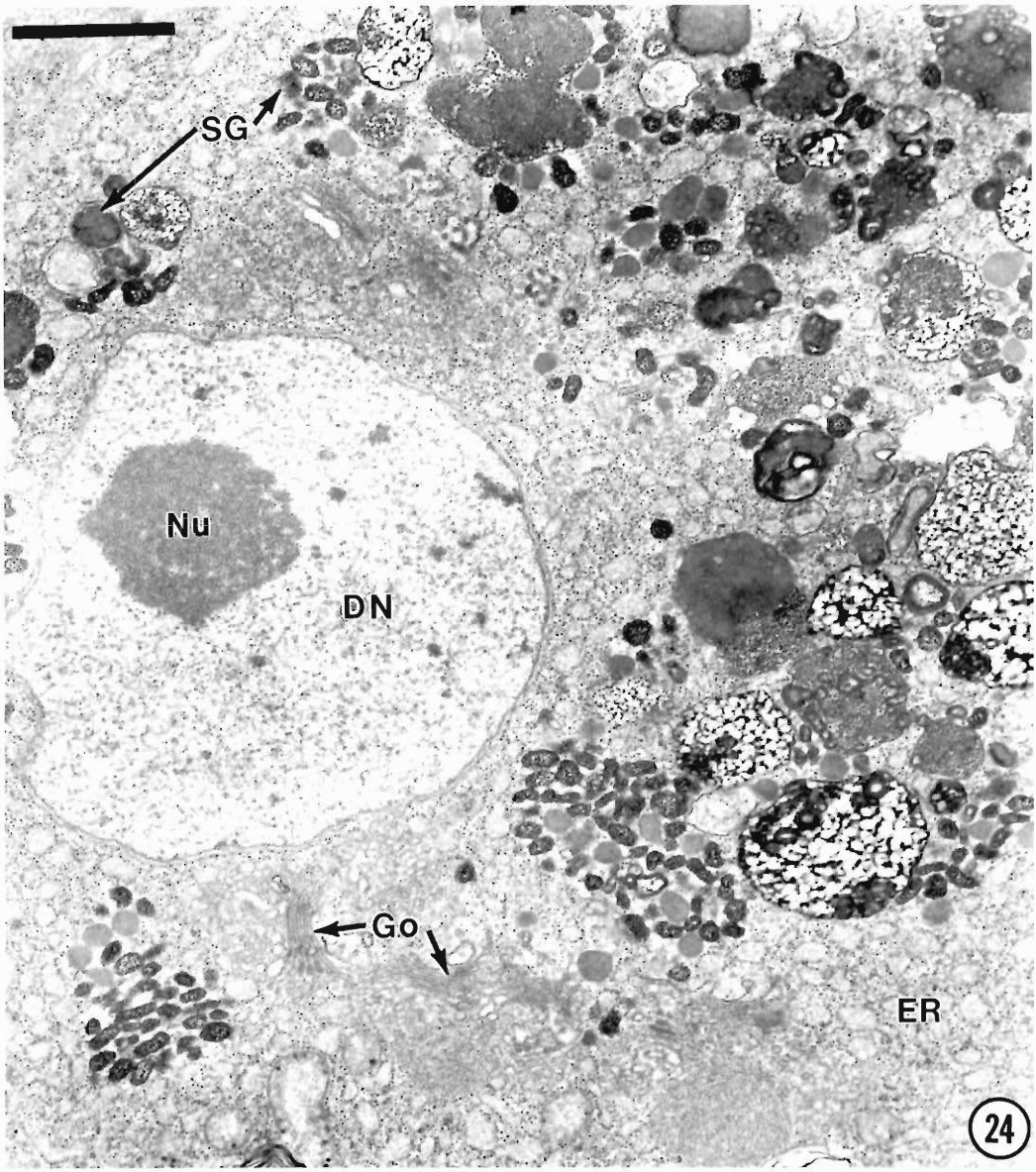

Figure 24. Longitudinal section of the midregion of dorsal gland shown in Figure 23. The dorsal gland nucleus (DN) is surrounded by numerous Golgi bodies (Go). The Golgi complexes receive newly synthesized protein and lipids from the endoplasmic reticulum (ER) and transfer them to plasma membranes, lysosomes and secretory granules (SG). Large secretory granules may form by condensation or aggregation of smaller secretory granules. Nu, nucleolus. Scale bar = 1.0 μm.

duct is cylindrical in shape. The LTSEM images of the tail region of a male specimen (Figs. 46, 47) can be compared to the thin-section images viewed in the transmission electron microscope (Fig. 44) and the micrographs by Wen and Chen (1976). The posterior lips of the cloaca and their embedded sensilla suggest a possible role in mating.

Discussion

The anterior sensory anatomy of *P. penetrans* was compared to that of other species of *Pra-*

tylenchus in an extensive study conducted with electron and scanning electron microscopy (Trett and Perry, 1985). The observations in our study are consistent with those made in other *Pratylenchus* spp. (Trett and Perry, 1985) as well as other species of Tylenchida (Baldwin and Hirschmann, 1973, 1975; De Grisse et al., 1974; McLaren, 1976; Wergin and Endo, 1976; Endo and Wergin, 1977; Endo, 1980). The protractor and anterior somatic muscles structurally interact with the cephalic framework, stylet knobs, and mitochondria-rich sarcoplasm of the protractor muscles. Similar complexity of tylenchid stylets was shown in ultrastructural studies of *Criconemoides curvatum* Raski, 1952 (Wen and Chen, 1972; Mai et al., 1977), *Meloidogyne incognita* (Kofoid and White, 1919) Chitwood, 1949 (Baldwin and Hirschmann, 1976), and *Heterodera glycines* Ichinohe, 1952 (Baldwin and Hirschmann, 1976; Endo, 1983).

The narrow, sinuous pathway of the dorsal gland extension, shown within the procorpus of Figures 5 and 7, illustrates a juvenile stage of a nematode or one that is not actively feeding. The gland extension of the nematode, shown in Figures 8 and 9, is enlarged and filled with numerous secretory granules whose presence is an indication of a very active host–parasite interaction. The ultrastructure and sometimes the chemical nature of secretory granules have been observed and studied in *Ditylenchus dipsaci* (Yuen, 1968), *Meloidogyne javanica* (Treub, 1885) Chitwood, 1949 (Bird and Saurer, 1967; Bird, 1968), *Heterodera schachtii* (Wyss et al., 1984), *Meloidogyne incognita* (Hussey, 1989; Hussey and Mims, 1990), and *Heterodera glycines* (Endo, 1993). The extensive change in the size of the dorsal gland extension and the associated ampullae of *P. penetrans*, as observed in our study, suggests that this species should also be considered for applying monoclonal body technology that is used in other species (Atkinson et al., 1988; Atkinson and Harris, 1989; Hussey, 1989; Davis et al., 1994).

The accumulation of secretory granules in the gland extensions is controlled by sphincter muscles at the anterior and posterior ends of the metacorpus. This muscle function of *Pratylenchus penetrans* was previously shown on film with the aid of video-enhanced light microscopy (Zunke and Institut für den Wissenschaftlichen Film, 1988). This observation is consistent with results found in other tylenchid species, including *Hexatylus viviparus* Goodey, 1952, *Aphelenchoides blastophthorus* Franklin, 1952, *Heterodera glycines*, and *Meloidogyne incognita* (Shepherd and Clark, 1976; Shepherd et al., 1980; Endo, 1984, 1987; Endo and Wergin, 1988). Secretory granules synthesized in the dorsal gland and confined within the dorsal gland extension of the metacorpus were relatively small and appeared uniform in size. However, granules of the same gland extension in the procorpus were greatly enlarged and varied widely in electron opacity. These cellular changes may be related to biochemical reactions that can lead to a better understanding of nematode feeding and host responses.

In transverse section, the short thick-walled metacorpus valve and pump muscles of *P. penetrans* appear similar to those of second-stage juveniles of *H. glycines* (Endo, 1984) but differ from juveniles of *Meloidogyne incognita* in which the metacorpus valves are thinner and more elongate (Endo and Wergin, 1988). The sphincter muscles at each end of the metacorpus

→

Figures 25, 26. Sections of subventral glands of *P. penetrans*. 25. Longitudinal section of a subventral gland of an adult male with Golgi bodies and numerous, small, moderately electron-opaque secretory granules (SG), some of which appear to condense into larger moderately dense granules. In contrast to the secretory granule formation and accumulation that occurs in the dorsal glands (Figs. 23, 24), the subventral glands have fewer, less electron-opaque and enlarged secretory granules. Go, Golgi; N, nucleus. 26. A cross-section of a subventral gland having an accumulation of secretory granules (SG) and convoluted nuclear (N) envelope. This gland is located at a narrow terminal region of a subventral gland adjacent to the intestinal epithelium. Go, Golgi; SED, secretory-excretory duct. Scale bars = 1.0 μm.

Figures 27, 28. Sections through intestinal regions of *P. penetrans*. 27. Longitudinal section of intestinal lumen (IL) partially occluded by evaginations of supporting membranes of the intestinal epithelial cells (IEc). N, nucleus. 28. Cross-section of an intestinal lumen (IL). Lumen wall is distended by microvilli-like membrane invaginations (MvL). Cell junctions (j) at boundary of lumen wall indicate bi-layered arrangement of cells comprising the intestinal epithelium. Scale bars = 1.0 μm.

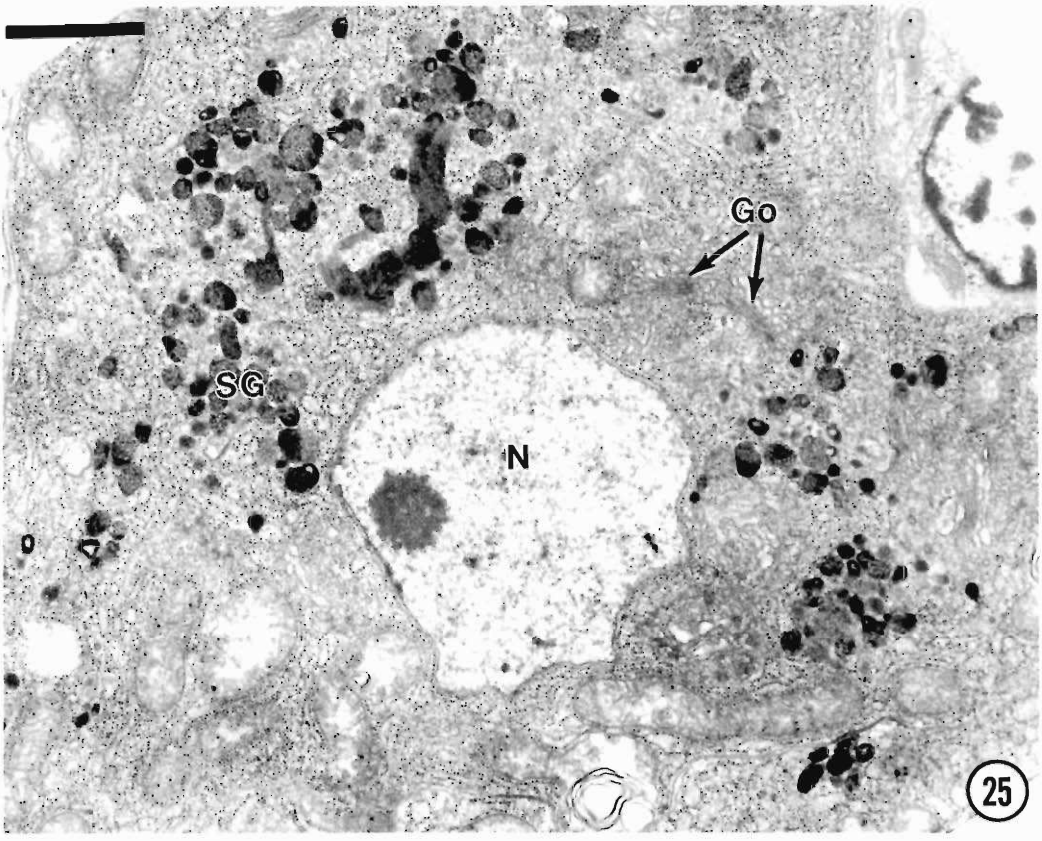

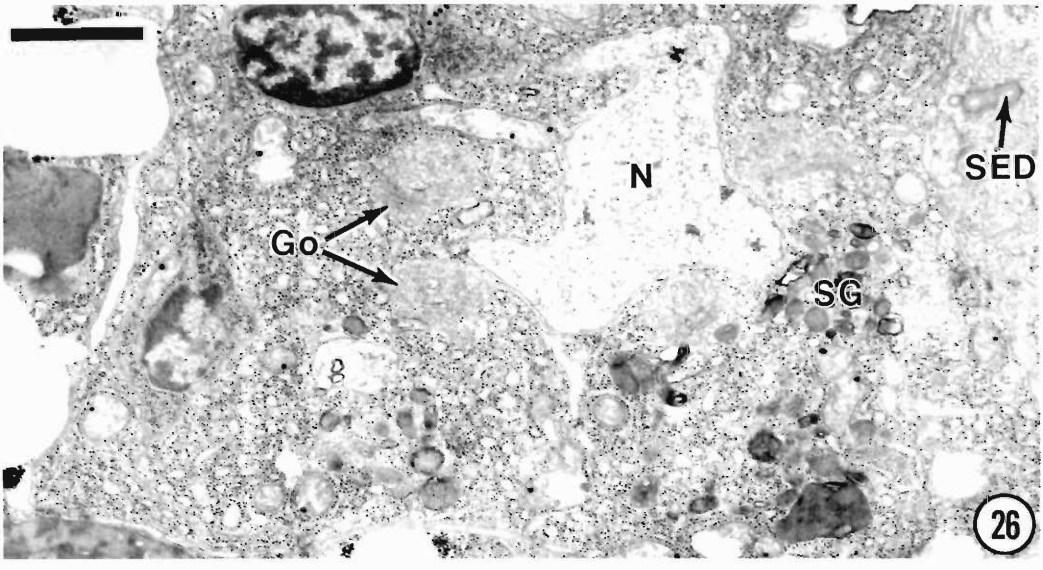

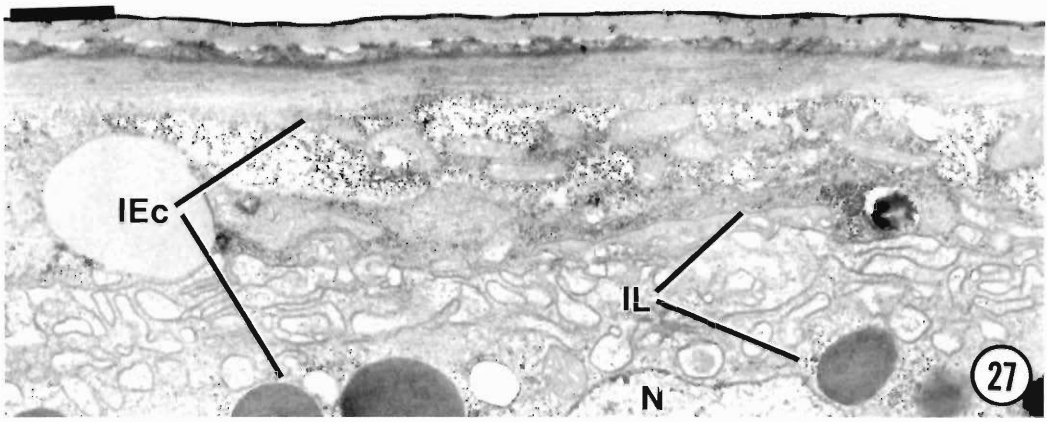

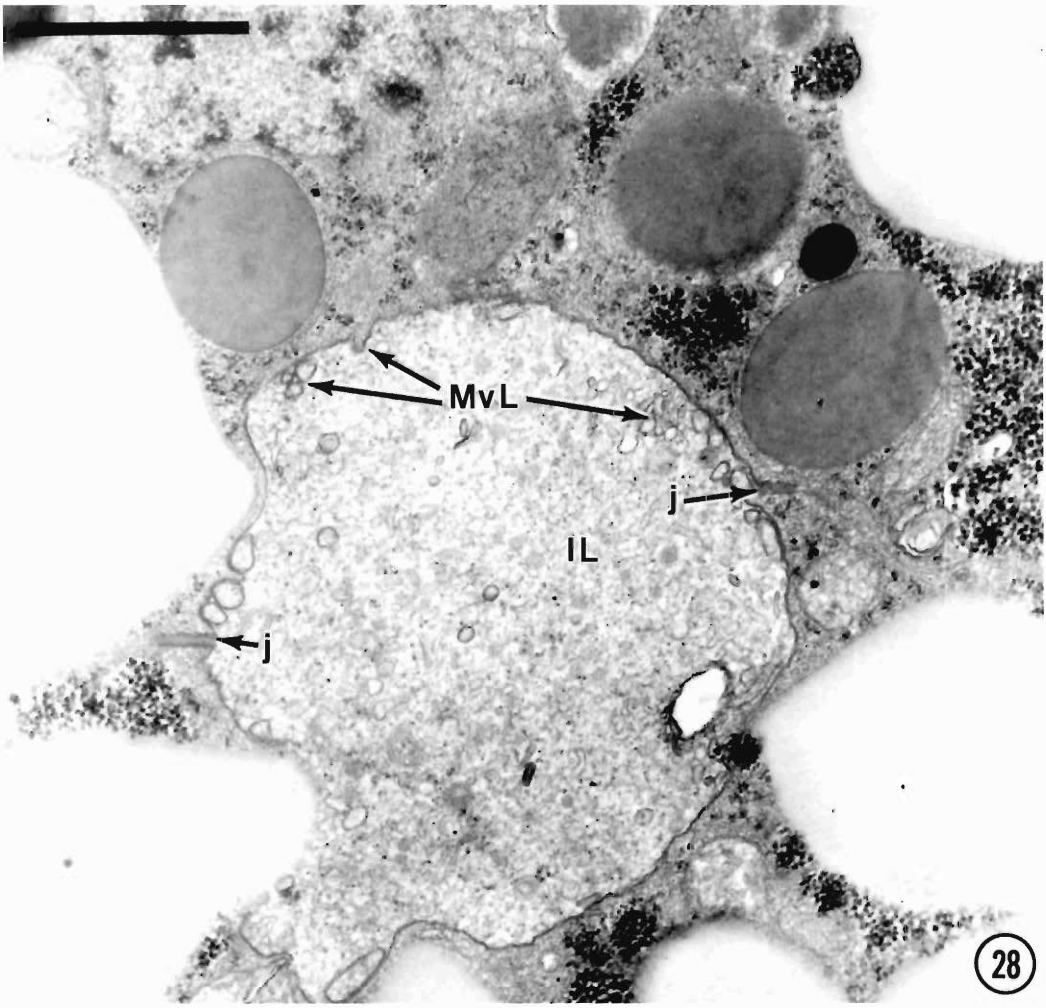

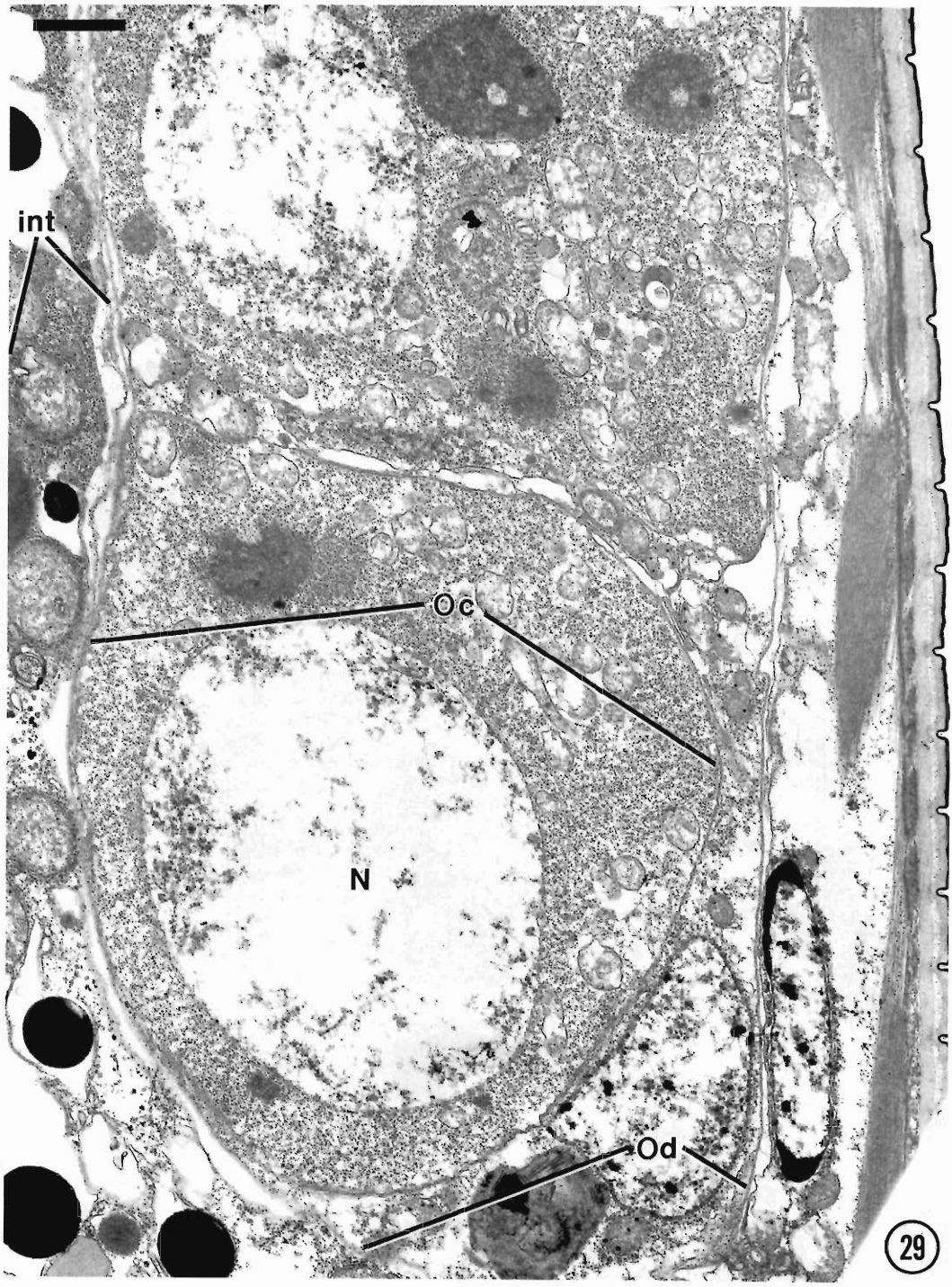

Figure 29. Longitudinal section of an adult female of *P. penetrans* showing oocytes (Oc) prior to their entry into the oviduct (Od), which may be occupied in actively reproducing females. int, intestine; N, nucleus. Scale bar = 1.0 μm.

are multidirectional internally and collar-shaped externally and appear to be in a position to open or close channels that lead from the dorsal and subventral glands (Endo, 1984). This functional role of sphincter muscles was demonstrated with video-enhanced light microscopy in which secretory materials from esophageal glands of *H. schachtii* flowed through ducts or was restricted from movement during feeding and quiescent periods (Wyss and Zunke, 1986). The asymmetrical appearance of the metacorpus and the adjoining organs of *P. penetrans*, which we observed with transmission electron microscopy, is consistent with the images that were obtained using LTSEM.

The dorsal and subventral gland extensions are part of the isthmus of the esophagus and are surrounded by the nerve ring. The dorsal gland cytoplasm contains numerous Golgi complexes that are involved with the formation and accumulation of secretory granules. More granules accumulate and condense in the dorsal gland than in the subventral gland. Future observations should correlate secretory activity with feeding and development as in the sedentary endoparasitic taxa, *Heterodera* and *Meloidogyne* (Wyss et al., 1985; Wyss and Zunke, 1986; Hussey and Mims, 1990).

In the juvenile stage, the intestinal lumen of *Pratylenchus penetrans* appeared occluded with membrane folds of the intestinal epithelium. However, in advanced stages of nematode development, the intestinal lumen appeared to have a few vesicles and tubular invaginations of the intestinal wall which are probably parts of intestinal microvilli. This observation contrasts with that of juveniles of *Globodera rostochiensis* (Wisse and Daems, 1968) and *Heterodera glycines* (Endo, 1988), in which intestinal lumina are lined with microvilli having enteric coatings. The microvilli of the anterior region of the vermiform *Aphelenchoides blastophthorus* are short and bulbous, whereas the microvilli of

→

Figure 30. Longitudinal section of an adult female of *P. penetrans* showing a cluster of spermatozoa (sp) within the spermatheca (spt). Sperm cells have dense chromatin surrounded by mitochondria (Mc) and residual strands of fibrillar bundles (f) observed in spermatids of the male gonad. Convoluted membranes (cvM) of the region posteriad to the spermatheca are components of the columnar cells (clc) of the uterus. Large electron-opaque secretory bodies (SG) probably contribute to the outermost egg membranes as eggs pass through the uterus. N, nucleus. Scale bar = 1.0 μm.

Figures 31, 32. Spermatheca and uterus of *P. penetrans*. 31. Cross-section of an oocyte in or near the spermatheca. Oocyte (Oc) contains lipid droplets (LD) and protein granules (Pgr). Spermathecal wall (sptW) encloses the oocyte. IE, intestinal epithelium; N, cell nucleus of the spermatheca wall. 32. Cross-section of columnar secretory cells of the female gonad. Large glandular cells have centrad orientation with adjacent lateral membranes joined into membrane junctions (MJ). The lumen (L) is formed by the basal membranes of the columnar cells. Secretory granules (SG) occur in various stages of assembly, accumulation, and condensation into large electron-opaque secretory granules that are probably destined to be deposited on eggs passing through the columella of the uterus. Scale bars = 1.0 μm.

Figures 33–36. Longitudinal sections through the uterus and vaginal regions of *P. penetrans*. 33. Columnar cells (clc) lie posteriad to the spermatheca (Fig. 30) and just anteriad from the terminal vestibule region of the uterus described in Figure 34. cvM, convoluted membrane; Mc, mitochondria; MJ, membrane junctions. 34. Terminal region of uterus is filled with electron-opaque material. The vaginal duct is lined by a thick cuticularized vaginal wall supported by lateral bands of muscles (M). Dilator muscles (dm) attached to the outer region of the vaginal cuticle by hemidesmosomes show anteriad and posteriad orientation of muscle elements. The vaginal wall extends from inside the uterus (u) to the body cuticle. 35. Longitudinal section of an extension of the uterus in Figure 34. The nonfunctional region of the uterus appears as a lipid-filled postvulval uterine branch (pub) with a terminal cap cell nucleus (cCN). 36. Tail region with convoluted membranes of the rectum (r). The cuticular wall forming the anal canal is continuous with the body cuticle (cu). an, anus. Scale bars = 1.0 μm.

Figure 37. Longitudinal view of male gonad of *P. penetrans* showing transition of spermatocytes to spermatids. Spermatocytes (spc) in testis are recognized as cells with nuclei limited by nuclear envelopes. During transition from spermatocyte to spermatid (smt), reduction division occurs, the nuclear envelope disappears, and the chromatin of the nucleus (N) becomes concentrated into a sphere surrounded by fibrillar bodies (fb). Spermatids become amoeboid and have membrane evaginations that appear as filopodia (fp). Nu, nucleolus. Scale bar = 1.0 μm.

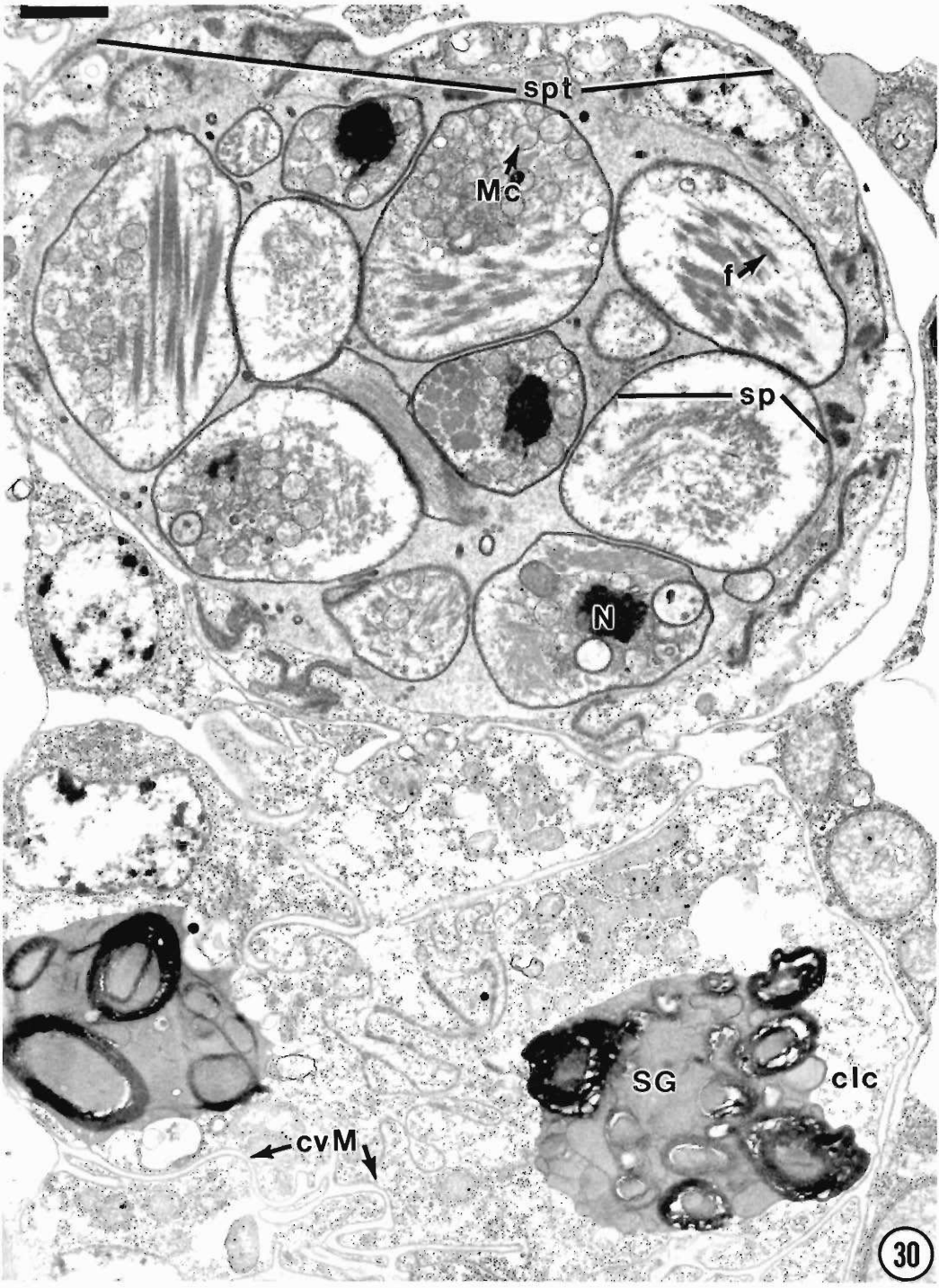

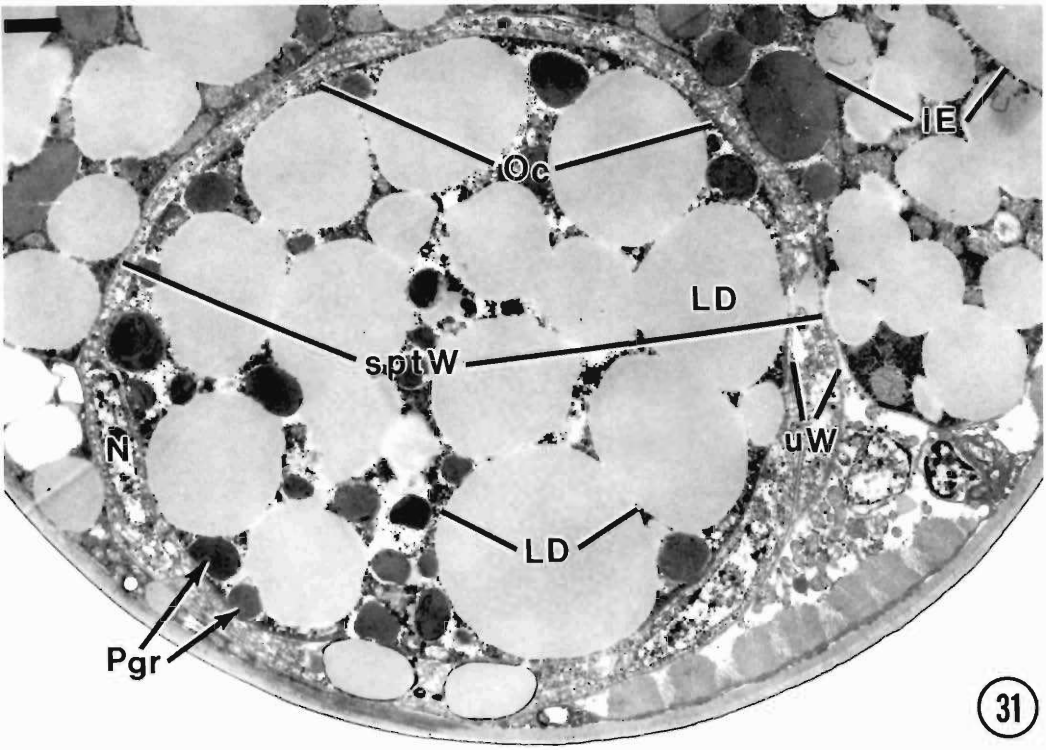

31

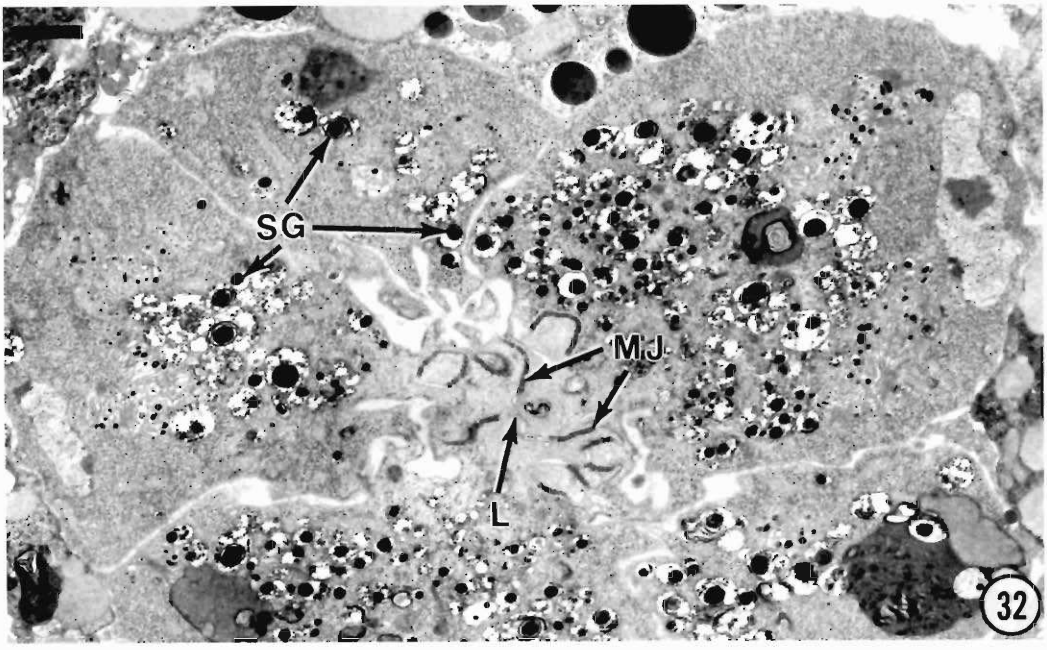

32

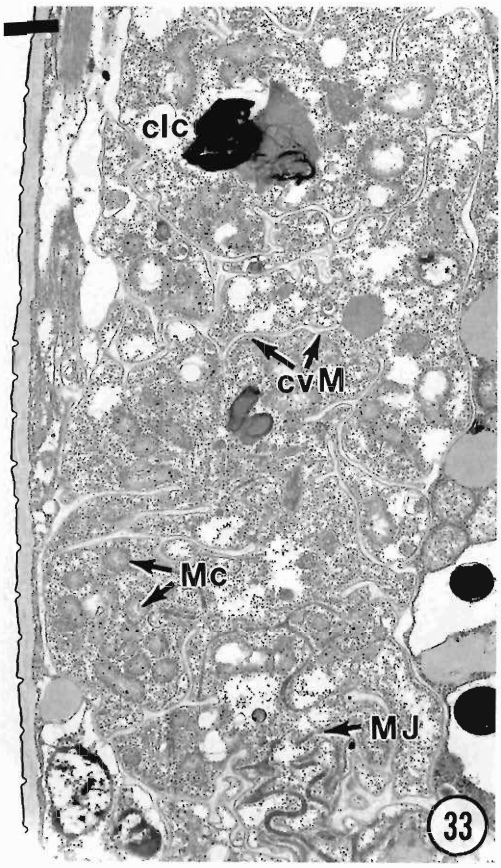

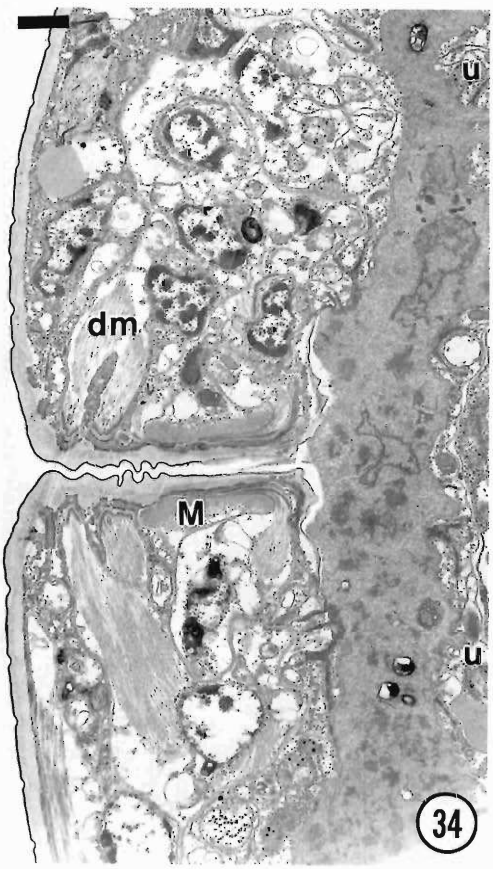

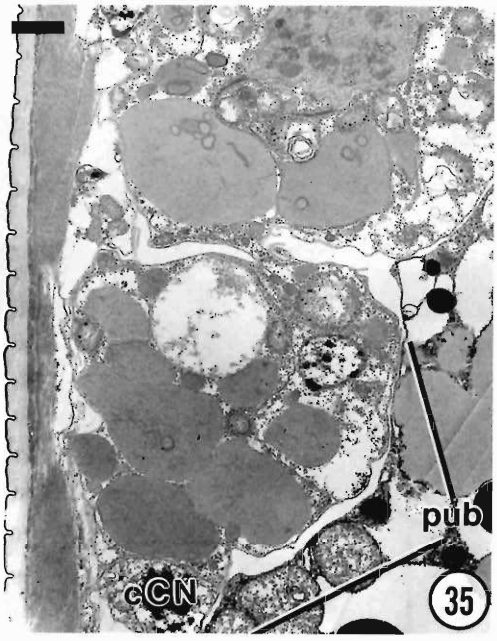

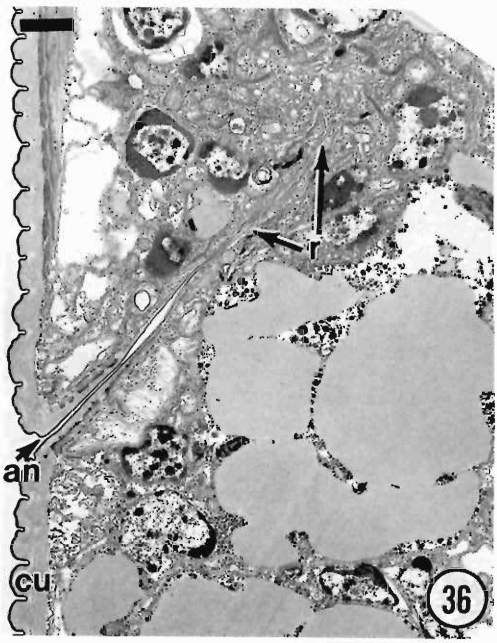

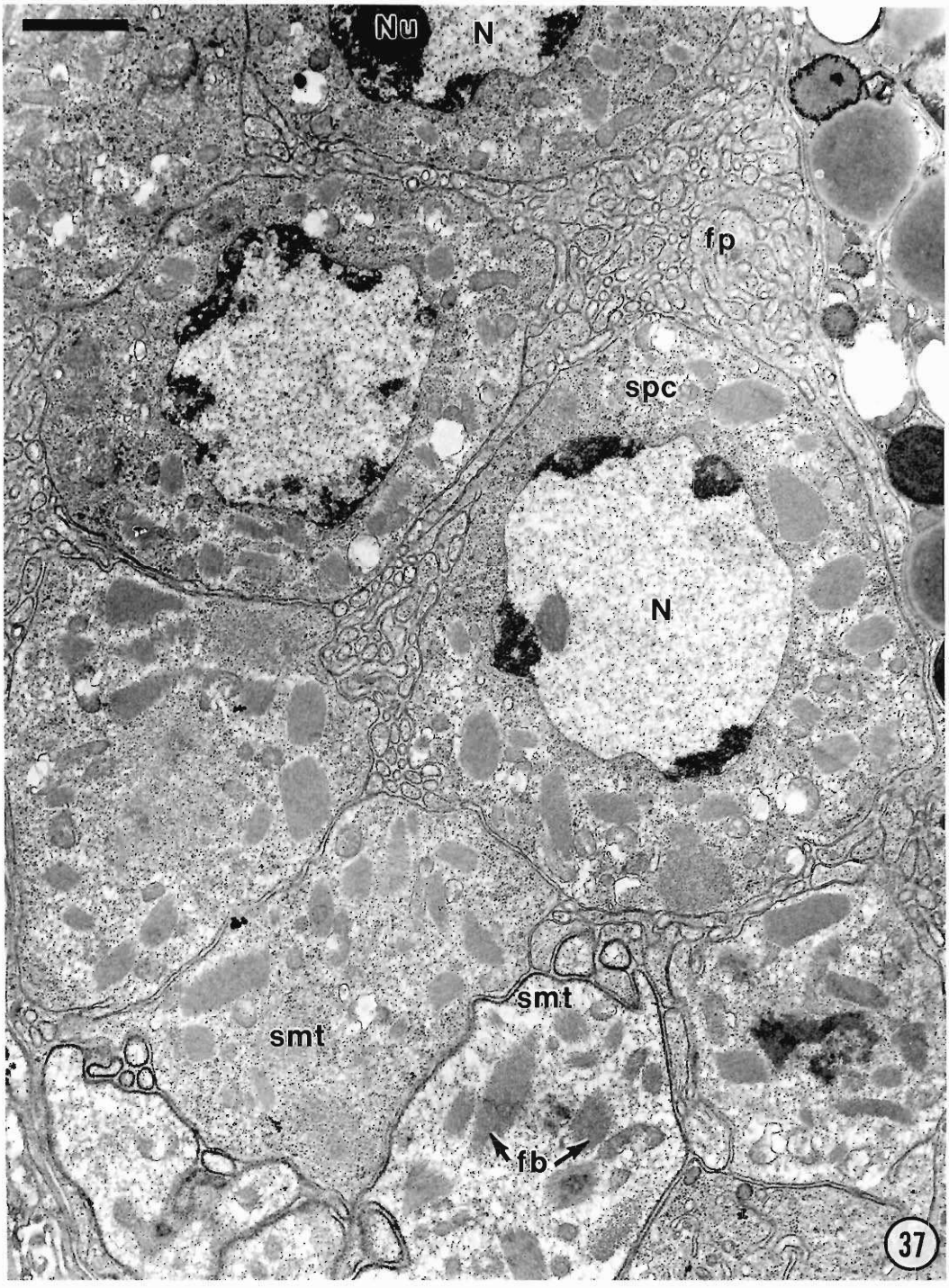

the midintestinal region are bottle-shaped (Shepherd et al., 1980).

Roman and Hirschmann (1969) studied the postembryonic development of gonads in several species of *Pratylenchus*. Most species, including *P. penetrans*, had the amphidelphic type of development in which 2 gonads developed up to the fourth stage, followed by deterioration of the posterior gonad. Thus, the reproductive system appears monodelphic. However, the only true monodelphic type observed was in *P. scribneri* Steiner, 1943. The authors concluded that all of the species, except *P. scribneri*, are potentially amphidelphic, that is, capable of developing a posterior gonad, which in some cases can be maintained in the adult stage. The present study of *P. penetrans* concurs with the monodelphic feature of the gonad; that is, the adult female gonad contains oocytes, an oviduct, spermatheca, columnar cells, a uterus, a vagina, a vulva opening, and a short postvulval uterine branch. According to Bird and Bird (1991), fertilization occurs near the junction between the oviduct and the uterus, where a spermatheca may or may not occur. Because *Pratylenchus penetrans* is an amphimictic species having a spermatheca, fertilization probably takes place as the oocyte passes through the sperm-filled spermatheca. Roman and Triantaphyllou (1969) studied the maturation and fertilization of *P. penetrans*, *P. vulnus* Allen and Jensen, 1951, and *P. coffeae* (Zimmerman, 1898) Filipjev and Schurrmans Stekhoven, 1941. Oocytes in the spermatheca contained a small number of bivalent chromosomes at prometaphase I. One spermatozoon entered each oocyte, which then rapidly completed the first division. At telophase I, the chromosomes that eventually formed the first polar body nucleus were discrete and were used to determine haploid chromosome numbers. A second maturation division followed rapidly, and the sperm pronucleus was formed, which in turn fused with the egg pronucleus to form the zygote nucleus. Actual fusion of the pronuclei was observed in nondeposited eggs of *P. penetrans* and in laid eggs of *P. coffeae*. According to Delves et al. (1986), the primary oocyte of *Dirofilaria immitis* (Leidy, 1956) Railliet and Henry, 1911, completes meiosis only after fertilization within the seminal vesicle by an entire male gamete. After meiosis I and II occurs in the oocyte and the 2 polar bodies are extruded, the haploid chromosome complement of the female unites with that of the male to reestablish the diploid number in the zygote. The spermatozoa of *P. penetrans* resembled those of *Heterodera* spp. (Shepherd et al., 1973), which were described as aflagellate, amoeboid, and lacking a nuclear membrane. The fibrillar bodies that are prominent in the spermatids appear as fibrillar residues in the clear region of spermatozoa. Ultrastructural studies of sperm development in the longidorid species, *Xiphinema theresiae* Stocker and Kruger, 1988, revealed the complexity of sperm morphology among a wide range of genera (Foor, 1970, 1983). In *X. theresiae*, the nonflagellated, slightly elongated spermatozoa are not polarized into head and tail regions. In cross-section, they have tightly packed chromosomes surrounded by perinuclear mitochondria without clear cristae, as well as bundles of microfilaments and membrane evaginations. Membrane

→

Figure 38. Section posteriad from that shown in Figure 37 illustrating maturing stage of spermatids (smt). Dense, electron-opaque chromatin of nuclei (N) is surrounded by dense clusters of fibrillar protein-like material (f). Spermatid wall membranes show convolutions that form pseudopodia and filopodia (fp). Closely packed spermatids (smt) have membrane boundaries that interdigitate with each other (→). Scale bar = 1.0 μm.

Figures 39, 40. Spermatids and spermatozoa in male gonad of *P. penetrans*. 39. Enlarged view of spermatids (smt) with electron-opaque spheroid nuclei (N). Seminal fluid is present between the tightly arranged spermatids in the seminal vesicle. Limiting membranes of spermatids have electron-opaque depositions (arrow). f, fibrillar body. 40. Gonad showing sperm (sp) within vas deferens. The nonmembrane-bound nuclei contain irregular clumps of chromatin (cr) surrounded by mitochondria (Mc). fp, filopodia; ps, pseudopodium. Scale bars = 1.0 μm.

Figures 41, 42. Cross-sections of tail region of male *P. penetrans*. 41. Section through base of spicules (Sp) that border terminal region of intestine (int) and related spicule protractor (Pm) muscles. 42. Sensilla (Se) components occur within curved arms of spicules (Sp) as they extend near the narrow lumen of the vas deferens (vdL). Pm, protractor muscles. Scale bars = 1.0 μm.

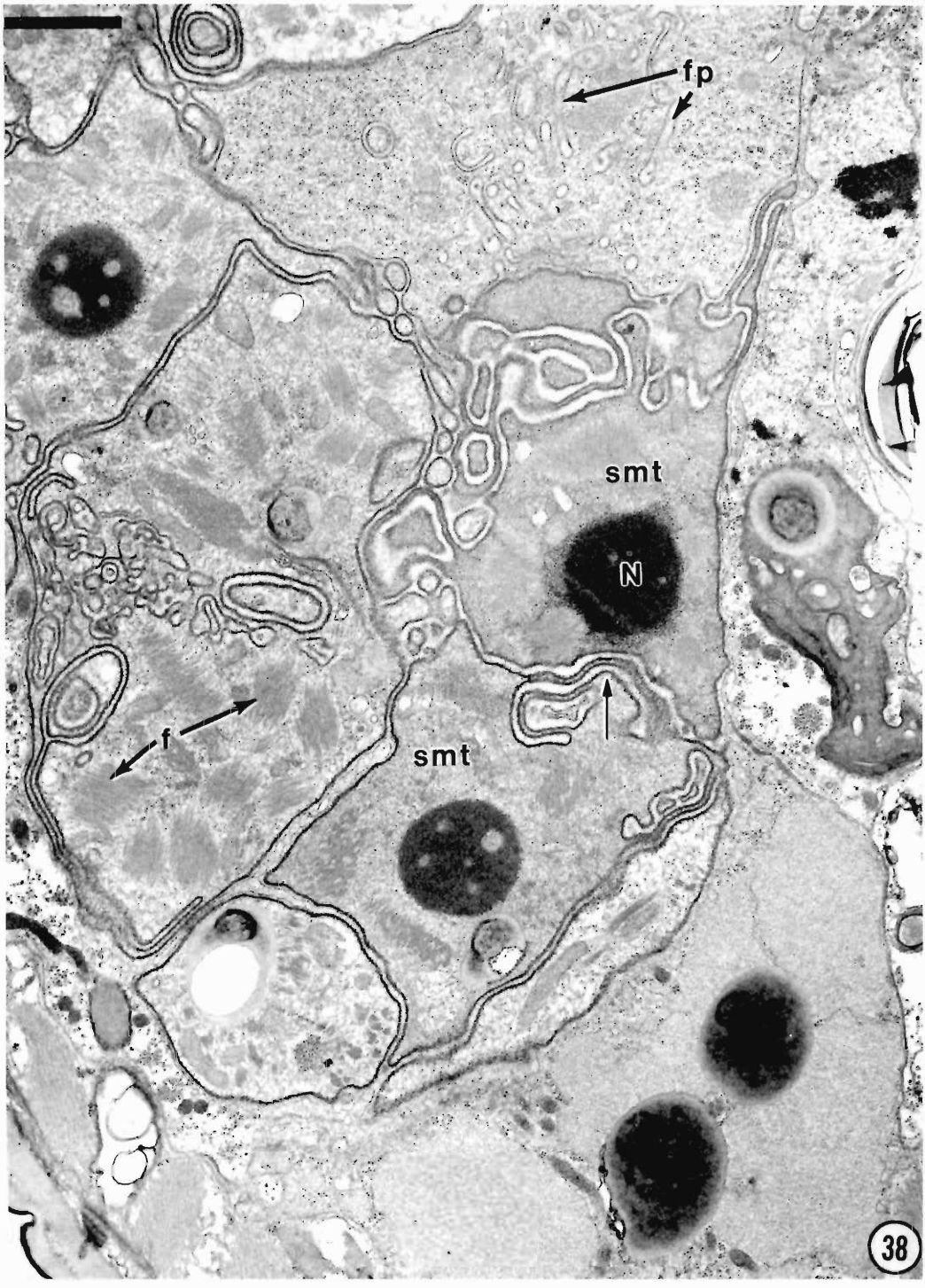

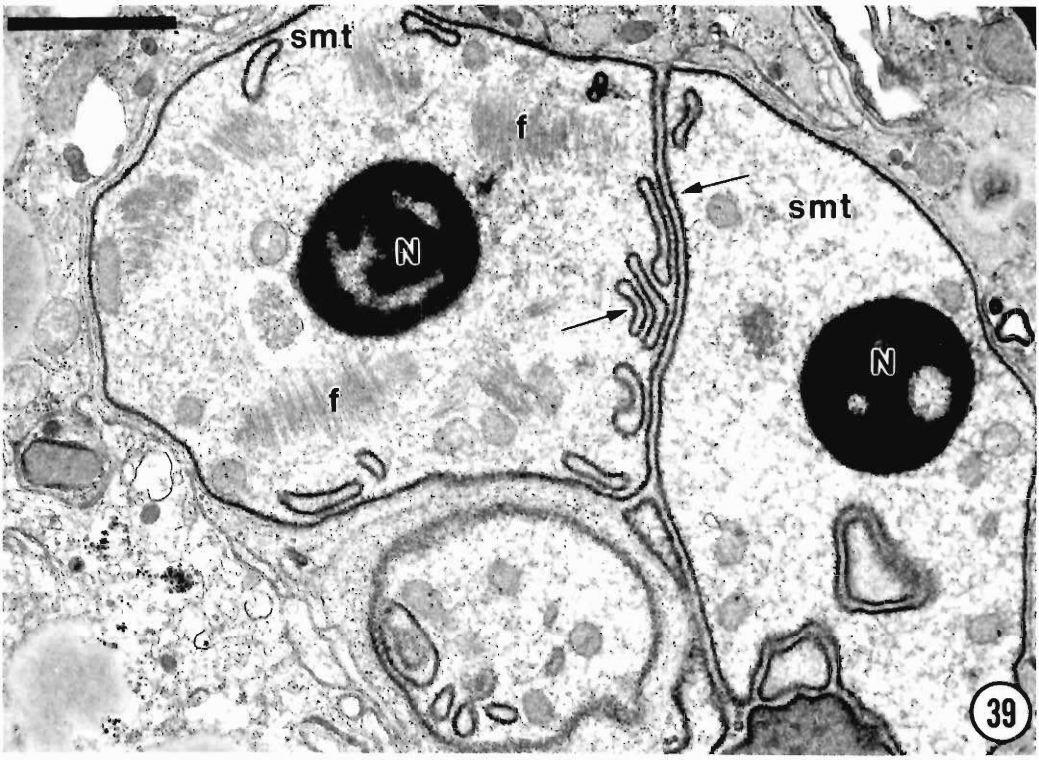

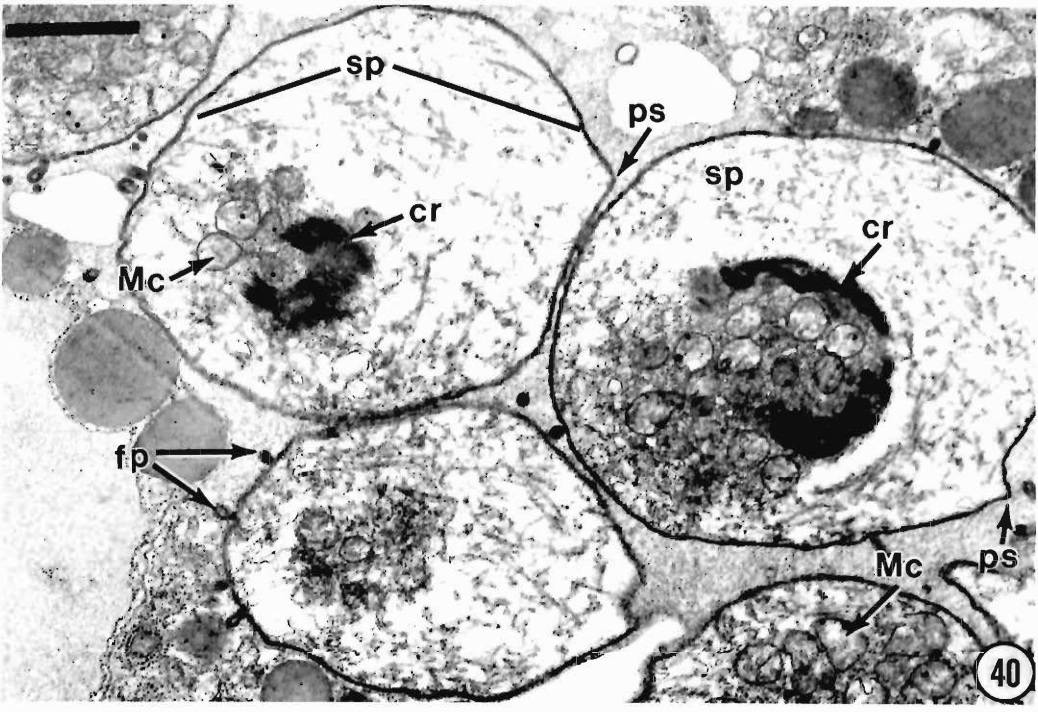

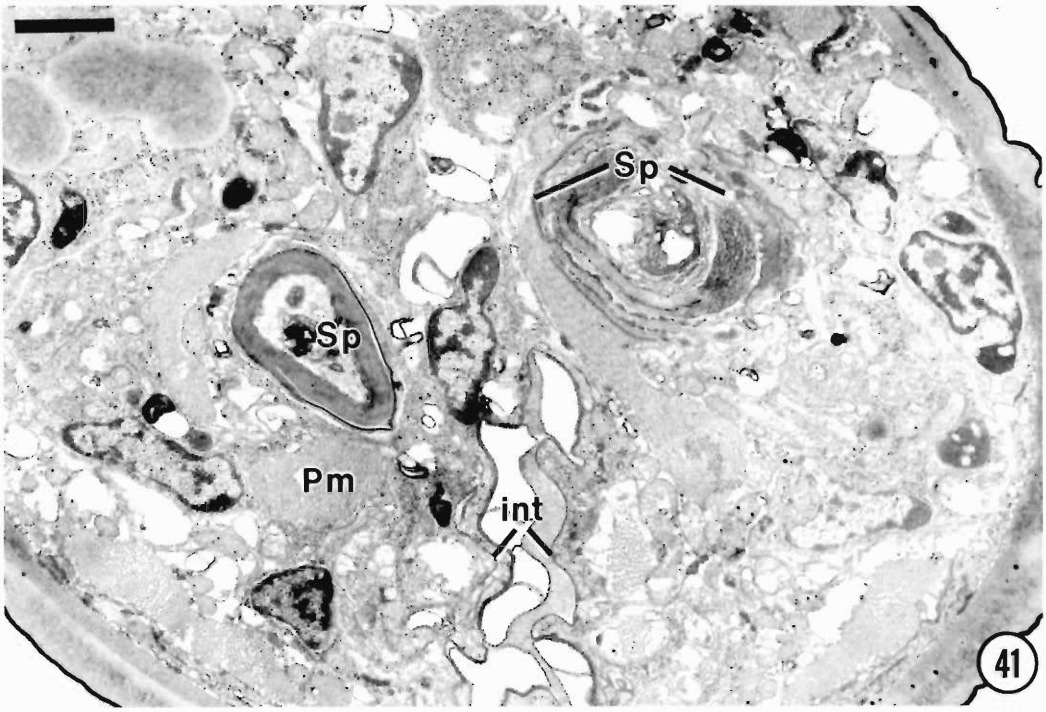

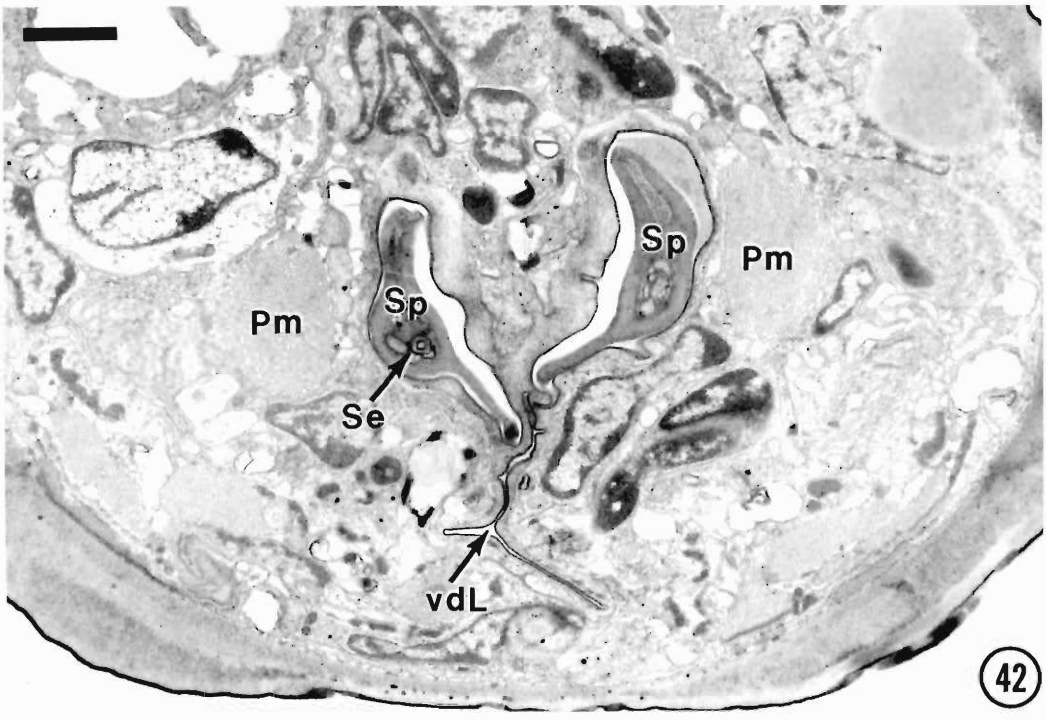

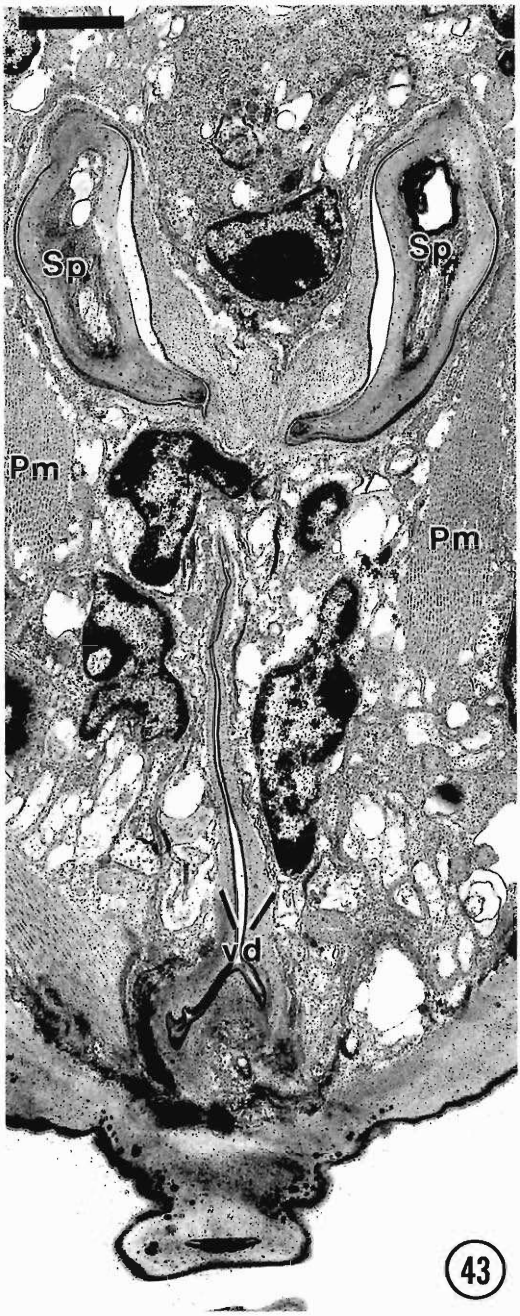

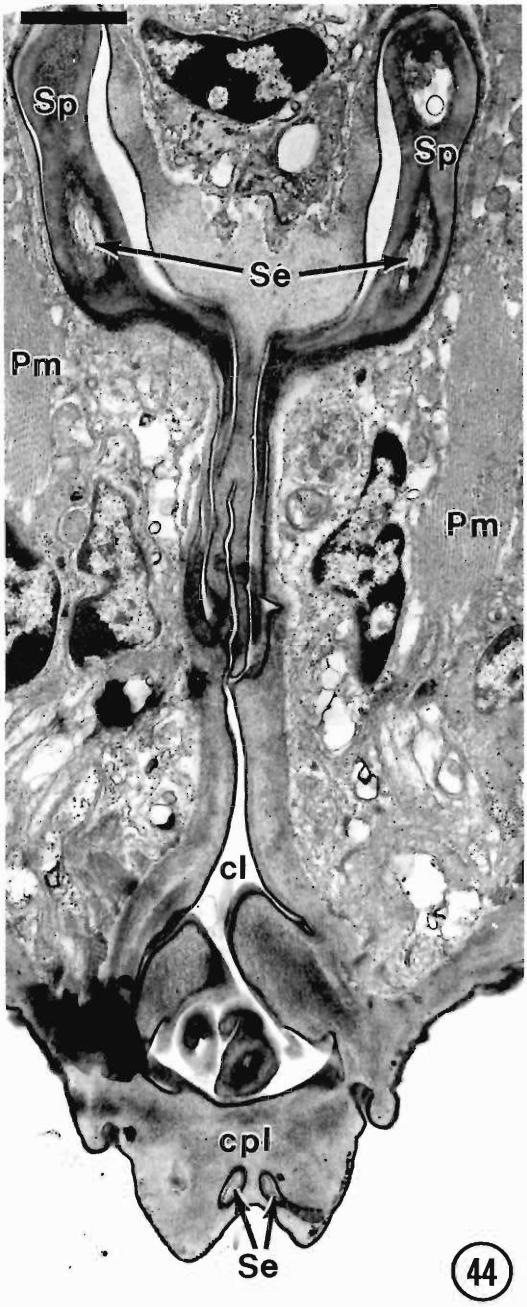

Figures 43, 44. Tangential sections showing spicule and cloacal regions of *P. penetrans*. **43.** Tangential orientation of tail region of specimen flanked by a pair of caudal alae (not shown). Vas deferens (vd) appears as an elongated slit that extends posteriad to the cloacal region. Vas deferens appears closed, is lined with cuticle and has a branched terminal zone. A pair of protractor muscles (Pm) extend posteriad from the dorsolateral region of the head or manubrium of the spicules (sp) and are assumed to be attached postanally on the body wall. **44.** Tangential section of same specimen illustrated in Figure 43 shows the retracted spicules (Sp) with sensilla (Se), protractor muscles (Pm), and part of the pathway for the extensible spicules. The cloaca (cl) is bordered terminally by posterior lips (cpl) that contain sensilla (Se). Scale bars = 1.0 μm.

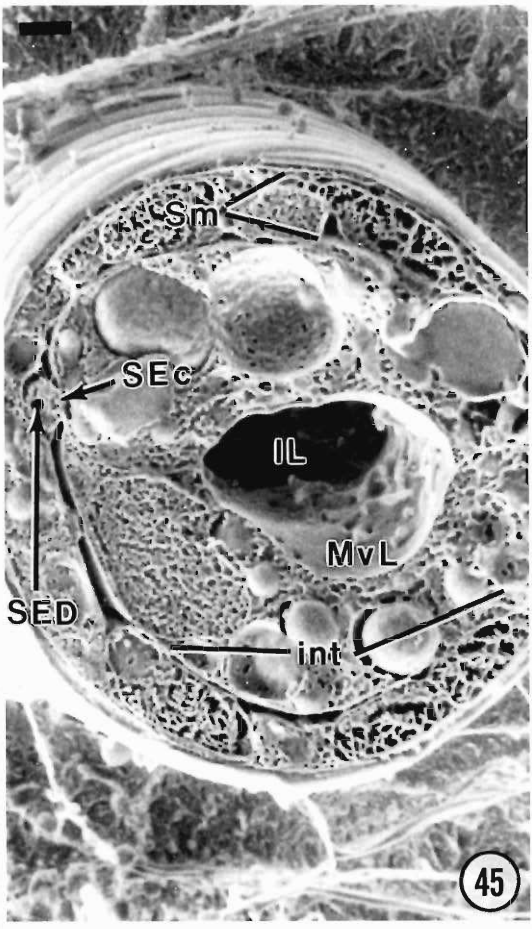

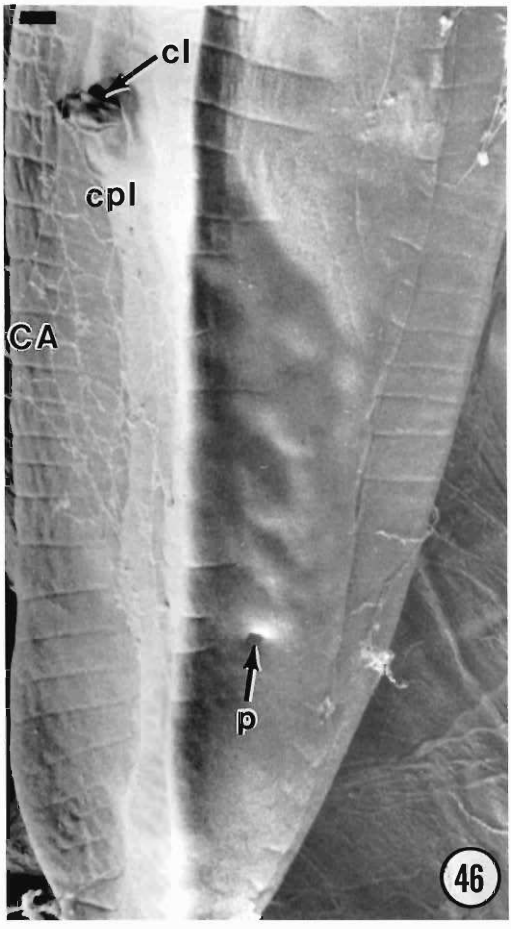

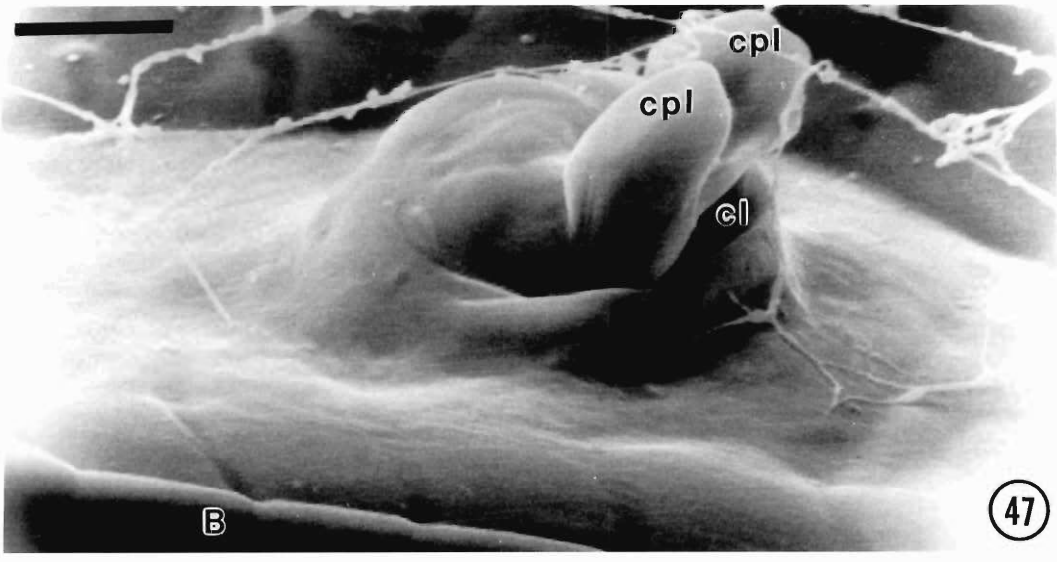

evaginations are pseudopodia (Kruger, 1991). Posteriad from the spermatheca of *P. penetrans*, columnar cells, also termed tricolumella, were reported to have a secretory function in that material they produce appeared to be deposited on the surface of the eggs. This concept is plausible considering the numerous secretory granules that occur in columnar cells of *P. penetrans*.

During oviposition, it is apparent that the large bands of dilator muscles attached to the cuticularized wall of the vagina play a significant role in the egg-laying process. In film, muscle movement was clearly visible near the opening of the vulva. This action occurred many hours before actual egg laying. The vulva was opened and closed by the dilator muscles of the vagina in a nonrhythmic manner and appeared to open more widely as egg-laying time approached (Zunke and Institut für den Wissenschaftlichen Film, 1988). The tooth-like cuticularized wall of the vagina (Fig. 34) may provide a degree of protection for the nematode by preventing the entry of foreign organisms into the vaginal canal. Similar tooth-like projections on the cuticular wall of the vagina were reported by Mai et al. (1977).

Study of the internal body structure of *P. penetrans* with LTSEM provides another means of observing nematode morphology that tends to verify the presence of chemically fixed structures observed with transmission electron microscopy. For example, the distorted image of the metacorpus from an adult *P. penetrans* observed with transmission electron microscopy is consistent with the image of cryofixed and freeze-fracture images obtained with LTSEM. Furthermore, the intestinal lumen of *P. penetrans* observed with transmission electron microscopy appeared disproportionately large within the body cavity in this and other species. However, this observation was also verified using LTSEM. This latter technology also enabled one to visualize the irregular membranous lining of the intestinal lumen in 3 dimensions (unpubl. obs.). Our observations of *P. penetrans* with LTSEM are consistent with those for *P. agilis* and *Steinernema carpocapsae* (Filipjev, 1934) (=*S. bibionis*, Bovien, 1937) in which the LTSEM was used to show surface and freeze-fractured images of these species (Wergin et al., 1993).

This ultrastructural overview of the lesion nematode indicates that there are many gaps in our knowledge of nematode developmental processes. Changes occurring in the esophageal glands that relate to feeding and the host–parasite interaction should be investigated. Because the lesion nematode is a pathogen by itself as well as a member of disease complexes with fungal pathogens, further studies on its feeding habits and host responses should yield information pertinent to disease management in crop plants.

Acknowledgments

The authors express appreciation to Sharon Ochs for technical support in specimen preparation for transmission electron microscopy, photographic processing, and preparing of final plates; Eric Erbe for preparation and recording of specimens observed with LTSEM; Naeema Latif for the maintenance and extraction of *Pratylenchus penetrans* used in the study; and Daniela Müller for technical support in Germany.

Literature Cited

Atkinson, H. J., and P. D. Harris. 1989. Changes in nematode antigens recognized by monoclonal antibodies during early infections of soya bean with the cyst nematode *Heterodera glycines*. Parasitology 98:479–487.

———, ———, **E. J. Halk, C. Novitski, J. Leighton-Sands, P. Nolan, and P. C. Fox.** 1988. Monoclonal antibodies to the soya bean cyst nem-

←

Figures 45–47. Low-temperature scanning electron micrographs of the intestine and tail region of *P. penetrans*. 45. Freeze-fracture and etched surface of intestinal region shows large intestinal lumen (IL) lined with microvilli-like invaginations (MvL) that are derived from supporting cells. Secretory-excretory cell (SEc) lying between the intestine (int) and somatic muscles (Sm) has a distinct tubular duct (SED). 46. Surface view of tail region of a male specimen showing the cloacal opening (cl) and its posterior lip (cpl) flanked on either side by caudal alae (CA) formed by body cuticle. The pore (p) of one of the paired phasmids is visible near the edge of the caudal ala and approximately a body-width anteriad from the tail terminus. 47. Enlargement of cloacal region of Figure 46 showing posterior lips of the cloaca (cpl) and opening (cl) where spicules emerge. B, bursa; CA, caudal alae. Scale bars = 1.0 μm.

atode, *Heterodera glycines*. Annals of Applied Biology 112:459–469.

Baldwin, J. G., and H. Hirschmann. 1973. Fine structure of cephalic sense organs in *Meloidogyne incognita* males. Journal of Nematology 5:285–302.

———, **and** ———. 1975. Fine structure of cephalic sense organs in *Heterodera glycines* males. Journal of Nematology 7:40–53.

———, **and** ———. 1976. Comparative fine structure of the stomatal region of males of *Meloidogyne incognita* and *Heterodera glycines*. Journal of Nematology 8:1–17.

Bird, A. F. 1967. Changes associated with parasitism in nematodes. I. Morphology and physiology of preparasitic and parasitic larvae of *Meloidogyne javanica*. Journal of Parasitology 53:768–776.

———. 1968. Changes associated with parasitism in nematodes. IV. Cytochemical studies on the ampulla of the dorsal esophageal gland of *Meloidogyne javanica* and on exudations from the buccal stylet. Journal of Parasitology 54:879–890.

———, **and J. Bird.** 1991. The Structure of Nematodes, 2nd ed. Academic Press, New York. 316 pp.

———, **and W. Saurer.** 1967. Changes associated with parasitism in nematodes. II. Histochemical and microspectrophotometric analyses of preparasitic and parasitic larvae of *Meloidogyne javanica*. Journal of Parasitology 53:1262–1269.

Cares, J. E., and J. G. Baldwin. 1994a. Comparative fine structure of sperm of *Verutus volvingentis* and *Meloidogyne floridensis* (Heteroderinae, Nematoda). Canadian Journal of Zoology 72:1481–1491.

———, **and** ———. 1994b. Fine structure of sperm of *Ekphymatodera thomasoni* (Heteroderinae, Nemata). Journal of Nematology 26:375–383.

Coomans, A., and A. T. De Grisse. 1981. Sensory structures. Pages 127–174 *in* B. M. Zuckerman and R. A. Rohde, eds. Parasitic Nematodes. Vol. 3. Academic Press, New York.

Davis, E. L., R. Allen, and R. S. Hussey. 1994. Developmental expression of esophageal gland antigens and their detection in stylet secretions of *Meloidogyne incognita*. Fundamental and Applied Nematology 17:255–262.

De Grisse, A. T. 1977. The ultrastructure of the nerves in the head of 22 species of plant parasitic nematodes belonging to 19 genera (Nematoda: Tylenchida). D.Sc. Thesis, University of Gent, Belgium. (In Dutch.)

———, **P. L. Lippens, and A. Coomans.** 1974. The cephalic sensory system of *Rotylenchus robustus* and a comparison with some other Tylenchids. Nematologica 20:88–95.

Delves, C. J., R. E. Howells, and R. J. Post. 1986. Gametogenesis and fertilization in *Dirofilaria immitis* (Nematoda: Filarioidea). Parasitology 92: 181–197.

Dropkin, V. H. 1989. Introduction to Plant Nematology. John Wiley & Sons, New York. 304 pp.

Endo, B. Y. 1980. Ultrastructure of the anterior neurosensory organs of the larvae of the soybean cyst nematode, *Heterodera glycines*. Journal of Ultrastructure Research 72:349–366.

———. 1983. Ultrastructure of the stomatal region of the juvenile stage of the soybean cyst nematode, *Heterodera glycines*. Proceedings of the Helminthological of Washington 50:43–61.

———. 1984. Ultrastructure of the esophagus of larvae of the soybean cyst nematode, *Heterodera glycines*. Proceedings of the Helminthological Society of Washington 51:1–24.

———. 1987. Ultrastructure of esophageal gland secretory granules in juveniles of *Heterodera glycines*. Journal of Nematology 19:469–483.

———. 1988. Ultrastructure of the intestine of second and third juvenile stages of the soybean cyst nematode, *Heterodera glycines*. Proceedings of the Helminthological Society of Washington 55: 117–131.

———. 1993. Ultrastructure of subventral gland secretory granules in parasitic juveniles of the soybean cyst nematode, *Heterodera glycines*. Journal of the Helminthological Society of Washington 60:22–34.

———, **and W. P. Wergin.** 1973. Ultrastructural investigation of clover roots during early stages of infection by root-knot nematode, *Meloidogyne incognita*. Protoplasma 78:365–379.

———, **and** ———. 1977. Ultrastructure of anterior sensory organs of the root-knot nematode, *Meloidogyne incognita*. Journal of Ultrastructure Research 59:231–249.

———, **and** ———. 1988. Ultrastructure of the second-stage juvenile of the root-knot nematode, *Meloidogyne incognita*. Proceedings of the Helminthological Society of Washington 55:286–316.

Foor, W. E. 1970. Spermatozoan morphology and zygote formation in nematodes. Biology of Reproduction Supplement 2:177–202.

———. 1983. Nematoda 2. Pages 221–256 *in* K. G. and R. G. Adiyodi, eds. Reproductive Biology of Invertebrates. Vol. II. Spermatogenesis and sperm function. John Wiley & Sons, New York.

Gamborg, O. L., T. Murashige, T. A. Thorpe, and I. K. Vasil. 1976. Plant tissue culture media. In Vitro 12:473–478.

Goverse, A., E. L. Davis, and R. S. Hussey. 1994. Monoclonal antibodies to the esophageal glands and stylet secretions of *Heterodera glycines*. Journal of Nematology 26:251–259.

Hussey, R. S. 1989. Monoclonal antibodies to secretory granules in esophageal glands of *Meloidogyne* species. Journal of Nematology 21:392–398.

———, **and C. W. Mims.** 1990. Ultrastructure of esophageal glands and their secretory granules in the root-knot nematode *Meloidogyne incognita*. Protoplasma 156:9–18.

———, **O. R. Paguio, and F. Seabury.** 1990. Localization and purification of a secretory protein from the esophageal glands of *Meloidogyne incognita* with a monoclonal antibody. Phytopathology 80:709–714.

Kruger, J. C. de W. 1991. Ultrastructure of sperm development in the plant-parasitic nematode *Xiph-*

inema theresiae. Journal of Morphology 210:163–174.

Mai, W. F., J. R. Bloom, and T. A. Chen. 1977. Biology and Ecology of the Plant-Parasitic Nematode *Pratylenchus penetrans.* Bulletin 815. Pennsylvania State University. Agricultural Experiment Station. University Park, Pennsylvania. 64 pp.

McLaren, D. J. 1976. Nematode sense organs. Pages 195–265 *in* B. Dawes, ed. Advances in Parasitology. Vol. 14. Academic Press, New York.

Roman, J., and H. Hirschmann. 1969. Embryogenesis and postembryogenesis in species of *Pratylenchus* (Nematoda: Tylenchidae). Proceedings of the Helminthological Society of Washington 36: 164–174.

———, **and A. C. Triantaphyllou.** 1969. Gametogenesis and reproduction of seven species of *Pratylenchus.* Journal of Nematology 1:357–362.

Rumpenhorst, H. J. 1984. Intracellular feeding tubes associated with sedentary plant-parasitic nematodes. Nematologica 30:77–85.

Shepherd, A. M., and S. A. Clark. 1976. Structure of the anterior alimentary tract of the passively feeding nematode, *Hexatylus viviparus* (Neotylenchidae: Tylenchida). Nematologica 22:332–342.

———, ———, **and A. Kempton.** 1973. Spermatogenesis and sperm ultrastructure in some cyst nematodes, *Heterodera* spp. Nematologica 19: 551–560.

———, ———, **and J. Hooper.** 1980. Structure of the anterior alimentary tract of *Aphelenchoides blastophthorus* (Nematoda: Tylenchida, Aphelenchina). Nematologica 26:313–357.

Spurr, A. R. 1969. A low-viscosity epoxy resin embedding medium for electron microscopy. Journal of Ultrastructure Research 26:31–43.

Townshend, J. L., and L. Stobbs. 1981. Histopathology and histochemistry of lesions caused by *Pratylenchus penetrans* in roots of forage legumes. Canadian Journal of Plant Pathology 3: 123–128.

———, ———, **and R. Carter.** 1989. Ultrastructural pathology of cells affected by *Pratylenchus penetrans* in alfalfa roots. Journal of Nematology 21:530–539.

Trett, M. W., and R. N. Perry. 1985. Functional and evolutionary implications of the anterior sensory anatomy of species of root-lesion nematode (genus *Pratylenchus*). Revue de Nématologie 8:341–355.

Wen, G. Y., and T. A. Chen. 1972. Ultrastructure of the feeding apparatus of *Criconemoides curvatum.* Phytopathology 62:501. (Abstract.)

———, **and** ———. 1976. Ultrastructure of the spicules of *Pratylenchus penetrans.* Journal of Nematology 8:69–74.

Wergin, W. P., and B. Y. Endo. 1976. Ultrastructure of a neurosensory organ in a root-knot nematode. Journal of Ultrastructure Research 56:258–276.

———, **R. M. Sayre, and E. F. Erbe.** 1993. Use of low temperature scanning electron microscopy to observe frozen hydrated specimens of nematodes. Journal of Nematology 25:214–226.

Wisse, E., and W. T. Daems. 1968. Electron microscopic observations on second-stage larvae of the potato root eelworm *Heterodera rostochiensis.* Journal of Ultrastructure Research 24:210–231.

Wyss, U. 1992. Observations on the feeding behavior of *Heterodera schachtii* throughout development, including events during molting. Fundamental and Applied Nematology 15:75–89.

———, **C. Stender, and H. Lehmann.** 1984. Ultrastructure of feeding sites of the cyst nematode *Heterodera schachtii* Schmidt in roots of susceptible and resistant *Raphanus sativus* L. oleiformis Pers. cultivars. Physiological Plant Pathology 25: 21–37.

———, **and U. Zunke.** 1986. Observations on the behavior of second stage juveniles of *Heterodera schachtii* inside host roots. Revue de Nématologie 9:153–165.

———, ———, **and Institut für den Wissenschaftlichen Film.** 1985. *Heterodera schachtii* (Nematoda). Behavior inside Roots (rape). Film E 2904. Encyclopaedia Cinematographica, Göttingen.

Yuen, P. H. 1967. Electron microscopical studies on *Ditylenchus dipsaci* (Kühn) I. Stomatal region. Canadian Journal of Zoology 45:1019–1033.

———. 1968. Electron microscopical studies of *Ditylenchus dipsaci.* II. Oesophagus. Nematologica 14:385–394.

Zunke, U. 1987. Contrast Enhancement—Nematological Applications. Pages 65–75 *in* O. Van Laere and L. de Vael, eds. Advanced Techniques in Microscopy. Applications in Biological and Agricultural Research. Flanders Technology International Symposium, 1987. Agricultural Research Center, Ghent Belgium. 1988.

———. 1990a. Ectoparasitic feeding behavior of the root lesion nematode, *Pratylenchus penetrans,* on root hairs of different host plants. Revue de Nématologie 13:331–337.

———. 1990b. Observations on the invasion and endoparasitic behavior of the root lesion nematode *Pratylenchus penetrans.* Journal of Nematology 22:309–320.

———, **and Institut für den Wissenschaftlichen Film.** 1988. Behaviour of the Root Lesion Nematode *Pratylenchus penetrans.* Film C 1676. Institut für den Wissenschaftlichen Film. Göttingen, West Germany.

———, **and R. N. Perry.** 1992. Evolutionary implications of different feeding strategies of plant parasitic nematodes. Pages 128–132 *in* F. J. Gommers and P. W. Th. Maas, eds. Proceedings of the 2nd International Congress of Nematology (SICN), Veldhoven, 1990.